Marine Pollution Bulletin 229 (2026) 119697

Contents lists available at ScienceDirect

Marine Pollution Bulletin

journal homepage: www.elsevier.com/locate/marpolbul

Unraveling the size-dependent toxicity mechanisms of polystyrene microplastics on coral symbiotic *Symbiodiniaceae*: Integrated physiological and transcriptomic perspectives

Jiayuan Liang [a,*,1], Yating Yang [a,1], Tianyi Niu [d,e], Zhicong Li [a], Zhuqing Liang [c], Mingyao Lu [a], Li Zhang [c], Yihe Feng [c], Sanqiang Gong [a], Kefu Yu [a,b,**]

[a] Guangxi Laboratory on the Study of Coral Reefs in the South China Sea, School of Marine Sciences, Guangxi University, Nanning, 530004, China
[b] Southern Marine Science and Engineering Guangdong Laboratory (Guangzhou), Guangzhou, 510030, China
[c] School of Resources, Environment and Materials, Guangxi University, Nanning, 530004, China
[d] State Key Laboratory of Regional and Urban Ecology, Research Center for Eco-Environmental Sciences, Chinese Academy of Sciences, Beijing, 100085, China
[e] University of Chinese Academy of Sciences, Beijing, 100049, China

ARTICLE INFO

Keywords:
Microplastic pollution
Symbiodiniaceae
Species-specific toxicity
Oxidative stress
Transcriptomic profiling

ABSTRACT

Microplastic (MP) pollution poses a growing threat to coral reef ecosystems, yet its direct effects on symbiotic *Symbiodiniaceae* remain poorly characterized. In this study, we investigated the size-dependent toxicity and underlying mechanisms of polystyrene microplastics (PS-MPs; 0.1, 1, and 10 μm) on three *Symbiodiniaceae* species-*Cladocopium goreaui*, *Durusdinium trenchii*, and *Symbiodinium natans*-representing distinct ecological niches. Among the tested sizes, 10 μm PS-MPs induced the most pronounced toxicity, significantly reducing algal growth rate, photosynthetic efficiency, and Chlorophyll a (Chl-a) content. These effects were accompanied by increased cell volume and enhanced accumulation of carbohydrates and lipids. Notably, *S. natans* exhibited partial recovery at later stages, whereas *C. goreaui* showed persistent inhibition. Exposure to 10 μm PS-MPs also elicited marked oxidative stress in all species, as evidenced by elevated superoxide dismutase (SOD) and malondialdehyde (MDA) levels, along with enhanced production of extracellular polymeric substances (EPS) and soluble proteins. Morphological analyses revealed PS-MP adhesion to algal surfaces, leading to membrane disruption, chloroplast damage, and stimulated EPS secretion. Transcriptomic profiling demonstrated size- and species-specific responses: under 0.1 μm PS-MPs, *D. trenchii* upregulated oxidative phosphorylation and the TCA cycle, whereas *S. natans* responded to 1 μm PS-MPs by activating purine metabolism and oxidative phosphorylation. In contrast, 10 μm PS-MPs downregulated ribosomal and photosynthetic genes, while upregulating fatty acid biosynthesis and antioxidant defense pathways. Collectively, these findings reveal that PS-MP toxicity is both size- and species-dependent, providing mechanistic insights into how MPs disrupt coral-algal symbiosis and undermine reef ecosystem resilience.

1. Introduction

Coral reef ecosystems are among the most biologically diverse and productive marine systems on Earth, despite developing in oligotrophic tropical and subtropical waters. This paradoxical productivity is largely sustained by the symbiotic association between reef-building corals and photosynthetic dinoflagellates of the family Symbiodiniaceae (Davy et al., 2012). These dinoflagellates, belonging to the order Suessiales (class Dinophyceae), have diversified into multiple genera, including *Symbiodinium*, *Breviolum*, *Cladocopium*, *Durusdinium*, *Effrenium*, *Fugacium*, and *Gerakladium* (LaJeunesse et al., 2018). Within coral tissues, *Symbiodiniaceae* fix inorganic carbon through photosynthesis and translocate up to 95% of their photosynthates to the coral host, thereby supporting host metabolism, calcification, and reef accretion (Torda et al., 2017; Putnam et al., 2017). Beyond their role as endosymbionts, *Symbiodiniaceae* also exist as abundant free-living populations in reef

* Corresponding author.
** Correspondence to: K. Yu, Southern Marine Science and Engineering Guangdong Laboratory (Guangzhou), Guangzhou, 510030, China.
E-mail addresses: jyliang@gxu.edu.cn (J. Liang), kefuyu@scsio.ac.cn (K. Yu).
[1] These authors contributed to the work equally and should be regarded as co-first authors.

https://doi.org/10.1016/j.marpolbul.2026.119697
Received 5 January 2026; Received in revised form 4 March 2026; Accepted 30 March 2026
Available online 6 April 2026

waters, sediments, and biofilms, where they function as primary producers and serve as a critical reservoir for symbiont acquisition by corals (Baird et al., 2009; Ali et al., 2019). Because most reef-building corals acquire their symbionts horizontally from the environment rather than through vertical transmission, the physiological condition and environmental persistence of free-living *Symbiodiniaceae* are essential for successful symbiosis establishment, coral recruitment, and post-disturbance recovery (Okubo et al., 2018). Consequently, stressors that impair the growth, photosynthesis, or stress tolerance of *Symbiodiniaceae* at the algal level may have cascading effects on coral health and reef ecosystem stability.

In recent decades, coral reef ecosystems have been increasingly threatened by a range of anthropogenic stressors, among which plastic pollution has emerged as a pervasive and growing concern. Global plastic production has increased nearly 200-fold since the 1950s, reaching approximately 368 million tonnes by 2019 (Gao et al., 2021). As plastics fragment and degrade, large quantities of microplastics (MPs; typically defined as plastic particles ranging from 100 nm to 5 mm) are released into marine environments (Collignon et al., 2014; Sana et al., 2020). Owing to their small size, persistence, and high surface-area-to-volume ratio, MPs can adsorb chemical contaminants and interact directly with microorganisms across multiple trophic levels, inducing oxidative stress, metabolic disturbance, growth inhibition, and altered community structure (Thompson et al., 2004; Rochman et al., 2014; Cole et al., 2016). Coral reef environments are recognized as hotspots of microplastic contamination. MPs have been widely detected in reef-associated waters, sediments, and coral tissues in regions such as the Great Barrier Reef, the Maldives, and the South China Sea (Rahman et al., 2023). Recent estimates suggest that shallow reefs in the Asia-Pacific region already contain billions of plastic particles, with projections indicating a rapid increase in the coming decades (Pinheiro et al., 2023). Previous studies have documented multiple adverse effects of MPs on corals, including tissue damage, reduced fertilization success, altered metabolism, impaired calcification, and increased disease susceptibility (Reichert et al., 2018, 2019; Lamb et al., 2018; Zhang et al., 2023). Importantly, these impacts are often size-dependent, with smaller particles penetrating tissues and larger particles causing physical abrasion, shading, and energetic stress (Berry et al., 2019).

Growing evidence indicates that MPs can also exert direct toxic effects on *Symbiodiniaceae*, independent of the coral host. Experimental studies have demonstrated that polystyrene microplastics (PS-MPs) and nanoplastics can inhibit algal growth, disrupt photosynthetic electron transport, induce oxidative stress, and alter gene expression profiles in multiple *Symbiodiniaceae* taxa (Ripken et al., 2020; Su et al., 2020; Marangoni et al., 2022; Jiang et al., 2025; Liang et al., 2025). Because *Symbiodiniaceae* underpin coral energy supply and stress tolerance, such algal-level impairments may reduce symbiont availability, weaken coral–algal mutualism, and increase reef vulnerability to additional stressors such as warming and eutrophication. Despite these advances, several critical knowledge gaps remain. In particular, the size-dependent toxicity mechanisms of microplastics on different *Symbiodiniaceae* species with contrasting ecological strategies are still poorly understood. Particle size influences not only cellular uptake and surface adhesion but also light availability, physical interference, and oxidative stress generation. Moreover, species-specific physiological traits may mediate differential sensitivity and adaptive responses to microplastic exposure, with important implications for coral resilience.

To address these gaps, the present study systematically investigates the size-dependent effects of polystyrene microplastics (0.1, 1, and 10 μm) on three representative *Symbiodiniaceae* species: *Cladocopium goreaui*, a dominant and widely distributed coral symbiont; *Durusdinium trenchii*, a stress-tolerant taxon often associated with thermally resilient corals; and *Symbiodinium natans*, a cosmopolitan free-living species (Hansen and Daugbjerg, 2009; Chen et al., 2020; Saad et al., 2022). By integrating physiological measurements, ultrastructural observations, and transcriptomic analyses over an 18-day exposure period, this study aims to elucidate the cellular and molecular mechanisms underlying microplastic toxicity in *Symbiodiniaceae*. The results provide mechanistic insights into how microplastic pollution may compromise algal health, disrupt coral–algal symbiosis, and ultimately threaten the resilience of coral reef ecosystems.

2. Materials and methods

2.1. Microalgae cultivation and reagents

C. goreaui, *D. trenchii* and *S. natans* used in this study were isolated from *Acropora pruinose* in Weizhou Island, *Galaxea fascicularis* and *Acropora tenuis* from Xisha Islands (Qin et al., 2023). Microalgae cultivation procedures are described in detail in the Supplementary materials (Text S1). PS-MPs suspensions with three sizes (0.1, 1, and 10 μm; 2.5% w/v) were purchased from Besle Technology Research Center (Tianjin, China). The PS-MPs were uniformly dispersed in water. The size and morphology of the PS-MPs are shown in Fig. S1.

2.2. Exposure experiment

The experiment comprised four groups: one control and three exposure groups treated with PS-MPs of 0.1 μm, 1 μm, and 10 μm in particle size, each conducted in triplicate. *Symbiodiniaceae* cultures in the logarithmic growth phase were transferred to 500 mL Erlenmeyer flasks for an 18-day exposure experiment. This study selected a particle size range of 0.1–10 μm, ranging from small particle size to particle size similar to all three algal cells (Qin et al., 2023; Liang et al., 2025), to comprehensively explore the toxic effects of microplastic particle size on *Symbiodiniaceae*. The initial theoretical cell density was set at 1.0×10^5 cells/mL, and the PS-MPs concentration was 25 mg/L. This exposure level was selected based on reported environmental concentrations (Shruti et al., 2021; Abinandan et al., 2023), which are likely underestimated in reality (Covernton et al., 2019; Lindeque et al., 2020), as well as previous experimental studies (Wang et al., 2023; Li et al., 2024). Most studies have employed concentrations ranging from 10 to 100 mg/L, showing that low concentrations (≈5 mg/L) of MPs can stimulate algal growth and photosynthesis, whereas higher concentrations (≈50 mg/L) inhibit both growth and photosynthetic activity (Podbielska and Szpyrka, 2023). Moreover, higher concentrations facilitate the observation of significant changes within a short period, enabling an effective assessment of the toxic effects arising from color differences in PS-MPs (Niu et al., 2026). Therefore, relatively higher concentrations facilitate the observation of significant changes within a short period, enabling an effective assessment of the toxic effects arising from particle sizes differences in PS-MPs (Thompson et al., 2024). Following inoculation, cultures were incubated on an illuminated growth rack at 25 ± 1 °C, with a light intensity of 90 $\mu mol \cdot m^{-2} \cdot s^{-1}$ under a 14 h:10 h light-dark cycle. To prevent algal sedimentation, flasks were manually agitated three times daily.

2.3. Parameter measurement

2.3.1. Cell density and size

Cell density and size were measured every 3 days throughout the 18-day experiment. Cell density was determined using an inverted optical microscope (ECLIPSE Ni-E, Nikon Corporation, Tokyo, Japan) and the hemocytometer counting method (n = 8–12). Cell size was assessed using the same inverted optical microscope, with 30 randomly selected cells measured per sample, and the average value was calculated (Lim et al., 2022).

2.3.2. Photosynthetic pigments and photochemical efficiency

To analyze changes in photosynthetic activity, photosynthetic pigments and photochemical efficiency (*Fv/Fm*) were measured every three days. Chl-a determination was conducted using the method described

(Ritchie, 2006); further details are provided in Supplementary materials Text S2. After dark adaptation for 30 min, the *Fv/Fm* of Symbiodiniaceae was measured using a PAM fluorometer (PAM-2500, Walz GmbH, Effeltrich, Germany).

2.3.3. Antioxidant enzyme activity and soluble protein levels

Antioxidant enzyme activity and soluble protein levels were measured on days 3, 9, and 15 of the exposure. A 15 mL sample was collected into a centrifuge tube, and crude enzyme extracts were prepared following the method described (Su et al., 2020). Superoxide dismutase (SOD) activity, malondialdehyde (MDA) concentration, and soluble protein (BCA) content in the supernatant were measured using commercial kits (A001, A003, and A045; Nanjing Jiancheng Bioengineering Institute, Nanjing, China), according to the manufacturer's instructions (Yang et al., 2022). Further details are provided in Supplementary materials Text S3.

2.3.4. Extracellular polymeric substances (EPS), total sugar and total lipid content

On the 3rd, 9th, and 15th days of the experiment, 10 mL of algal suspension was collected for the measurement of EPS. The EPS quantification was performed following previously reported methods (Li et al., 2020a). Additional details are provided in Supplementary materials Text S4.

After 18 days of MPs exposure, 10 mL of algal suspension was collected into a centrifuge tube, centrifuged to remove the supernatant, and the total sugar content of the samples was measured using the sulfuric acid-anthrone method (Yemm and Willis, 1954). To measure total lipid content after 18 days of MPs exposure, 100 mL of algal suspension was centrifuged at 4000 $\times g$ for 5 min at 4 °C using a refrigerated centrifuge (Avanti J-26S XP, Beckman Coulter, Brea, CA, USA) (Ryckebosch et al., 2012). Further details are provided in Supplementary materials Text S5.

2.4. Ultrastructural analysis

On the 18th day of the experiment, algal suspensions were collected for morphological examination. Scanning electron microscopy (SEM) was employed to analyze the interactions between algal cells and PS-MPs, as well as to observe the surface morphology of *C. goreaui*, *D. trenchii*, and *S. natans*, using a field-emission scanning electron microscope (SU8010, Hitachi High-Tech Corporation, Tokyo, Japan). Transmission electron microscopy (TEM) was utilized to examine the internal structural morphology of *C. goreaui*, *D. trenchii*, and *S. natans* cells using a transmission electron microscope (JEM-1400Plus, JEOL Ltd., Tokyo, Japan). Detailed procedures are provided in Supplementary materials Text S6.

2.5. RNA extraction and transcriptomic analysis

Cells of *C. goreaui*, *D. trenchii*, and *S. natans* exposed to PS-MPs (0.1, 1, and 10 μm) for 18 days were collected by centrifugation. The control group was designated as Control, while the PS-MPs-treated groups were labeled as TR01 (0.1 μm), TR1 (1 μm), and TR10 (10 μm). The samples were immediately flash-frozen in liquid nitrogen and sent to Majorbio Biopharm Technology Co., Ltd. (Shanghai, China) for sequencing. Among them, *C. goreaui* and *S. natans* were analyzed with reference to high-quality genomes, whereas *D. trenchii* was not. Detailed transcriptomic analysis methods are described in Supplementary materials Text S7.

2.6. Statistical analysis

Raw data were processed using Excel, and significance among different groups on the same day was analyzed using SPSS. All datasets were first subjected to a normality test (Shapiro–Wilk test) and a homogeneity of variance test (Levene's test). When these assumptions were satisfied, a one-way analysis of variance (ANOVA) was conducted to assess overall differences among treatments. If the ANOVA revealed significant effects, Tukey's HSD post hoc test was applied for pairwise comparisons ($p < 0.05$). Figures were generated with Origin, and all results are presented as the mean ± standard error of the mean (SEM).

3. Results

3.1. Effects of PS-MPs on the growth and photosynthesis of C. goreaui, D. trenchii, and S. natans

3.1.1. Growth performance

The growth rate provides a straightforward indicator of algal cell damage. During the 18-day exposure experiment, PS-MPs of 0.1 μm and 1 μm exerted no detectable effects on the growth of the three algal species (Fig. 1A–C). In contrast, 10 μm PS-MPs resulted in significant growth inhibition across all species ($p < 0.05$), although the magnitude of this effect was clearly species dependent. *C. goreaui* exhibited the most severe response, with cell density reduced by more than 90% by day 18, followed by *D. trenchii* (approximately 70% reduction), whereas *S. natans* showed a comparatively moderate decline (approximately 30%). In addition to growth suppression, 10 μm PS-MPs induced a significant enlargement of algal cell size in all three species ($p < 0.05$; Fig. 1D–F), with clear interspecific differences in both the timing and extent of this response. The mean cell size of *C. goreaui* peaked at 9.82 ± 0.06 μm on day 12 (vs. 8.32 ± 0.18 μm in the control), *D. trenchii* reached 14.07 ± 0.81 μm on day 15 (vs. 10.56 ± 0.68 μm in the control), and *S. natans* attained 12.76 ± 0.04 μm on day 12 (vs. 10.81 ± 0.44 μm in the control). Scatter plots based on random measurements of 100 cells from the 10 μm PS-MPs treatment, together with optical microscopy observations, further revealed that approximately half of the algal cells exhibited an enlarged morphology (Fig. 1G–I).

3.1.2. Photosynthetic capacity

Photosynthesis in *Symbiodiniaceae* plays a pivotal role in maintaining symbiotic functionality. During the 18-day stress experiment, no significant differences in Maximum quantum yield of photosystem II (*Fv/Fm*) were observed between the control and the 0.1 μm or 1 μm PS-MPs treatments (Fig. 2A–C). In contrast, exposure to 10 μm PS-MPs significantly suppressed *Fv/Fm* in all three algal species ($p < 0.05$), with the most pronounced reduction detected in the environmentally sensitive species *C. goreaui*.

Photosynthetic pigments are essential for sustaining photosynthetic capacity. Throughout the 18-day exposure, 0.1 μm and 1 μm PS-MPs initially enhanced chl-a content in *C. goreaui* and *D. trenchii*, whereas no significant effect was observed in *S. natans* (Fig. 2D–F). However, exposure to 10 μm PS-MPs led to a marked decline in chl-a content across all species, albeit with distinct temporal patterns. In *C. goreaui*, chl-a levels dropped significantly below the control from day 3 onward and continued to decline throughout the exposure period (Fig. 2D). By contrast, *D. trenchii* and *S. natans* exhibited significant decreases during the early and mid stages, but chl-a content recovered to control levels by day 18 (Fig. 2E–F).

3.2. Oxidative stress induced by PS-MPs exposure in C. goreaui, D. trenchii, and S. natans

When algal cells are exposed to a toxic environment, their oxidative defense mechanisms are activated, while oxidative damage begins to accumulate. Compared with the control, exposure to 0.1 μm and 1 μm PS-MPs did not significantly affect SOD activity in *C. goreaui*, *D. trenchii*, or *S. natans* (Fig. 3A–C). In contrast, 10 μm PS-MPs markedly increased SOD activity in all three algae. Specifically, SOD activity in *C. goreaui* and *S. natans* remained significantly higher than the control throughout the exposure period, whereas in *D. trenchii*, a significant increase was

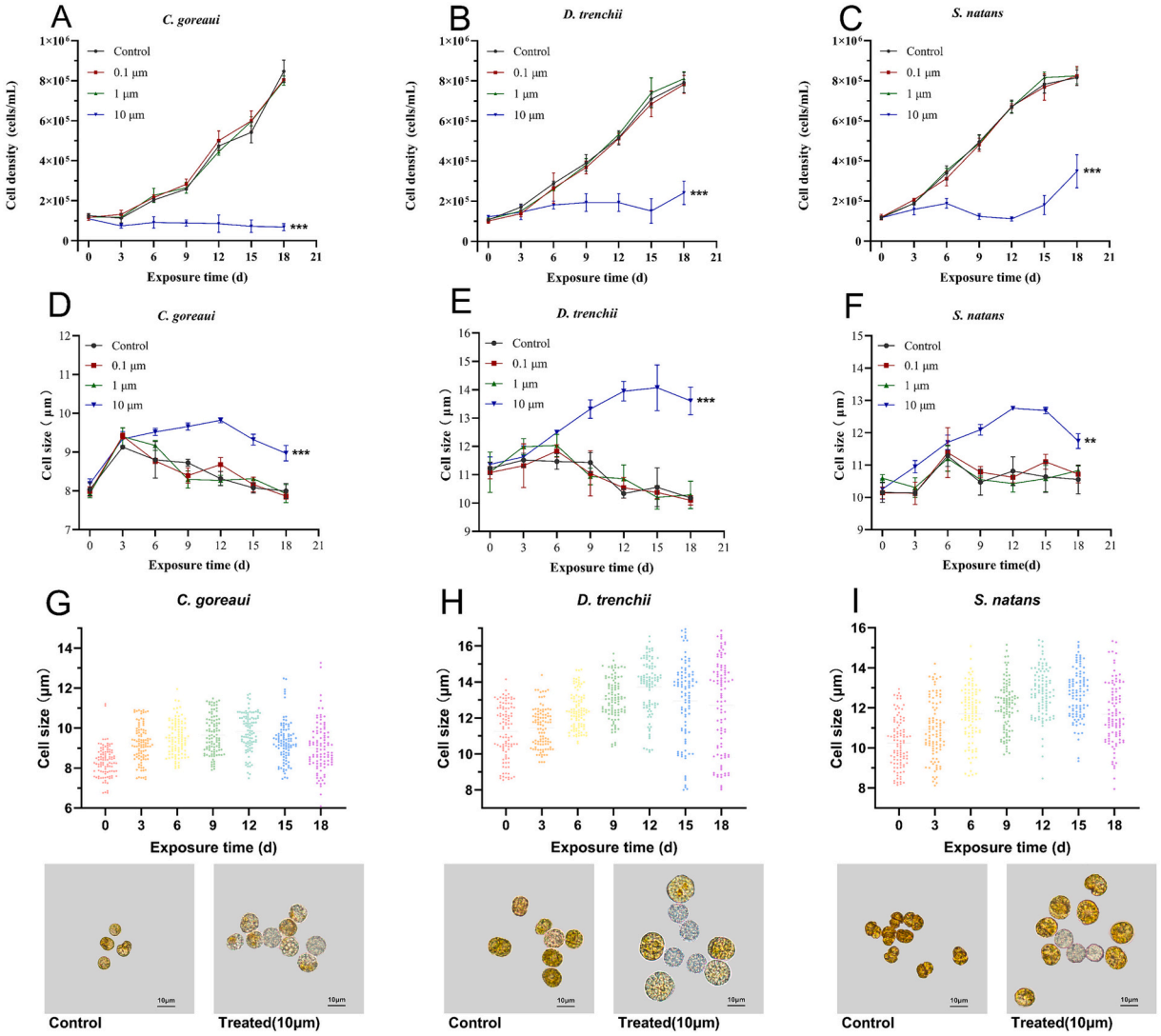

Fig. 1. Effects of PS-MPs of different particle sizes on the growth of *C. goreaui*, *D. trenchii*, and *S. natans*. (A–C) Cell density over the 18-day exposure period: (A) *C. goreaui*; (B) *D. trenchii*; (C) *S. natans*. (D–F) Changes in cell size: (D) *C. goreaui*; (E) *D. trenchii*; (F) *S. natans*. (G–I) Scatter plots of cell size and representative cell morphology images: (G) *C. goreaui*; (H) *D. trenchii*; (I) *S. natans*. Data points and bars represent the mean ± standard error of three biological replicates. The significance between the experimental group and the control group is indicated by asterisks (**: $p < 0.01$, ***: $p < 0.001$).

observed only on day 15.

MDA content increased in all PS-MP treatments relative to the control (Fig. 3D–F). Notably, exposure to 10 μm PS-MPs induced a rapid and sustained elevation of MDA levels. In *C. goreaui*, MDA reached 14.58 ± 1.52 nmol·7/cell on day 15, 6.33-fold higher than the control. In *D. trenchii*, the peak MDA was 111.98 ± 24.94 nmol·7/cell (4.07-fold), while *S. natans* reached 177.60 ± 5.08 nmol·7/cell (3.61-fold). These results indicate that PS-MPs of 0.1 μm, 1 μm, and 10 μm can induce oxidative damage in *C. goreaui*, *D. trenchii*, and *S. natans*, with 10 μm PS-MPs causing more severe lipid peroxidation and sustained oxidative stress, suggesting that the antioxidant defense system could not efficiently scavenge excessive reactive oxygen species (ROS) in algal cells.

EPS plays a protective role against toxic compound invasion. Although EPS content slightly increased in *D. trenchii* and *S. natans* exposed to 0.1 μm and 1 μm PS-MPs, 10 μm PS-MPs exposure resulted in more than a twofold increase in EPS content (Fig. 3G–I).

3.3. Impact of PS-MPs exposure on intracellular metabolites of *C. goreaui, D. trenchii, and S. natans*

Soluble proteins are essential cellular nutrients and play a key role in osmotic regulation. Although exposure to 0.1 μm and 1 μm PS-MPs initially stimulated *C. goreaui* and *D. trenchii* to produce more soluble proteins, overall, exposure to 10 μm PS-MPs led to a several-fold increase in soluble protein content across all three algal species (Fig. 4A–C). Compared with the control, soluble protein levels in the 10 μm group increased by 3.08-fold in *C. goreaui* on day 9, by 3.98-fold in *D. trenchii* on day 15, and by 2.66-fold in *S. natans* on day 9.

After 18 days of exposure, only 10 μm PS-MPs significantly ($p < 0.05$) enhanced the total sugar and lipid contents in all three algal species (Fig. 4D, E). Specifically, the total sugar content in *C. goreaui*, *D. trenchii*, and *S. natans* increased by 751.86%, 77.38%, and 48.85%, respectively, relative to the control, while total lipid content increased by 654.86%, 362.83%, and 277.48%, respectively.

3.4. Ultrastructural analysis

SEM and TEM images clearly reveal both the surface and internal morphology of the algal cells. After 18 days of cultivation, PS-MPs aggregated with *C. goreaui*, *D. trenchii*, and *S. natans*, forming substantial amounts of EPS (Fig. 5). These EPS not only contained PS-MPs and high-molecular-weight substances such as extracellular polysaccharides

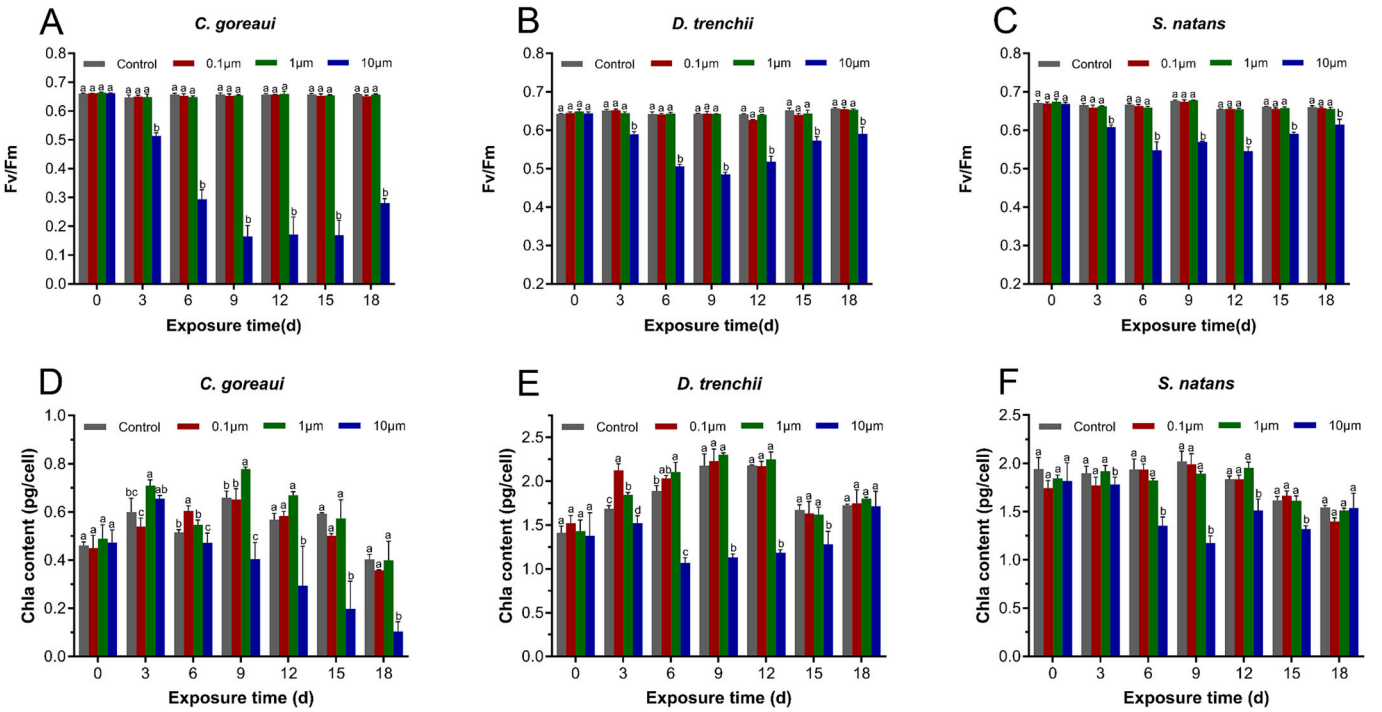

Fig. 2. Effects of PS-MPs of different particle sizes on the photosynthesis of *C. goreaui*, *D. trenchii*, and *S. natans*. (A–C) Maximum quantum yield of photosystem II (*Fv/Fm*); (A) *C. goreaui*; (B) *D. trenchii*; (C) *S. natans*. (D–F) Chlorophyll a (Chl-a) content; (D) *C. goreaui*; (E) *D. trenchii*; (F) *S. natans*. Bars represent the mean ± standard error ($n = 3$ biological replicates). Different letters (a, b, c, d) indicate statistically significant differences between groups ($p < 0.05$).

but also encapsulated a large number of symbiotic bacteria.

TEM analysis showed that 0.1 μm and 1 μm PS-MPs had minimal effects on the internal morphology of *C. goreaui*, *D. trenchii*, and *S. natans* cells (Fig. 6). In contrast, exposure to 10 μm PS-MPs caused notable damage to the chloroplasts of all three algae and induced phenomena such as cell shrinkage, deformation, and plasmolysis (Fig. 6D, H, L). In particular, the sensitive *C. goreaui* cells exhibited disintegration of both chloroplasts and nuclei. Furthermore, all three algal species displayed varying degrees of cytoplasmic vesicle proliferation. In addition, starch accumulation within the cells increased across all three algae (Fig. S2D–F).

3.5. Transcriptomic analysis

3.5.1. RNA-seq quality control

The quality control of the transcriptome sequencing data yielded 95.28 Gb, 88.28 Gb, and 87.79 Gb of high-quality data for *C. goreaui*, *D. trenchii*, and *S. natans*, respectively, with each sample containing at least 6.56 Gb of high-quality reads. The sequencing error rate ranged from 0.0117% to 0.0121% (all <0.1%), and the proportion of Q30 bases exceeded 95.91%, indicating that the sequencing data were of high quality and suitable for subsequent analyses (Tables S1-S3).

3.5.2. Venn diagram analysis of differentially expressed genes (DEGs) and gene ontology (GO) functional annotation

After 18 days of exposure to PS-MPs, the 10 μm treatment group exhibited the highest number of DEGs in *C. goreaui*, *D. trenchii*, and *S. natans*. Notably, *D. trenchii* and *S. natans* predominantly showed downregulated DEGs, whereas *C. goreaui* primarily displayed upregulated DEGs (Fig. S3). *C. goreaui* shared 4 DEGs across the 0.1 μm, 1 μm, and 10 μm groups, with 1575 DEGs being unique to the 10 μm group (Fig. 7A). *D. trenchii* exhibited 58 shared DEGs among the three groups and 48,433 DEGs unique to the 10 μm group (Fig. 7B). *S. natans* had 1 shared DEG across the three groups and 1142 DEGs unique to the 10 μm group (Fig. 7C). The gene expression patterns induced by 0.1 μm and 1 μm PS-MPs were relatively similar, whereas exposure to 10 μm PS-MPs resulted in more pronounced transcriptional differences.

GO functional annotation of DEGs in the three algal species encompassed biological processes, cellular components, and molecular functions, with a substantial number of DEGs enriched in "response to stimulus" and "catalytic activity" (Fig. 7D–F). Notably, in the 10 μm treatment groups of *C. goreaui* and *S. natans*, most DEGs within the cellular component category were enriched in "cellular anatomical entity"; however, DEGs related to detoxification were predominantly enriched in *C. goreaui*, whereas those associated with antioxidant activity were mainly enriched in *S. natans* (Fig. 7D, F). For *D. trenchii*, a larger proportion of DEGs in the cellular component category of the 10 μm group were enriched in "membrane," "organelle," "organelle part," and "membrane part" (Fig. 7E).

3.5.3. KEGG enrichment analysis of DEGs

For *C. goreaui* exposed to PS-MPs, the 0.1 μm and 10 μm treatment groups exhibited KEGG pathways that were either uniquely upregulated, uniquely downregulated, or showed both up- and downregulated DEGs, with significant enrichment observed in lipid metabolism-related pathways (Fig. 8A, C). In contrast, in the 1 μm treatment group, the up- and downregulated DEGs were distributed across different KEGG pathways, and no significantly enriched pathways were detected (Fig. 8B). Specifically, the 0.1 μm group showed marked enrichment in glycine, serine and threonine metabolism, fatty acid elongation, as well as valine, leucine, and isoleucine biosynthesis pathways (Fig. 8A). In contrast, the 10 μm group exhibited significant enrichment in pathways related to ribosome, photosynthesis, and fatty acid biosynthesis (Fig. 8C).

For *D. trenchii*, exposure to PS-MPs did not result in any KEGG pathways enriched exclusively by uniquely downregulated DEGs across the three treatment groups (Fig. 8D–F). The 0.1 μm and 1 μm groups contained pathways enriched solely by upregulated DEGs (Fig. 8D, E), whereas the 10 μm group exhibited pathways with both up- and downregulated DEGs (Fig. 8F). Notably, the 0.1 μm group was also significantly enriched in oxidative phosphorylation and the

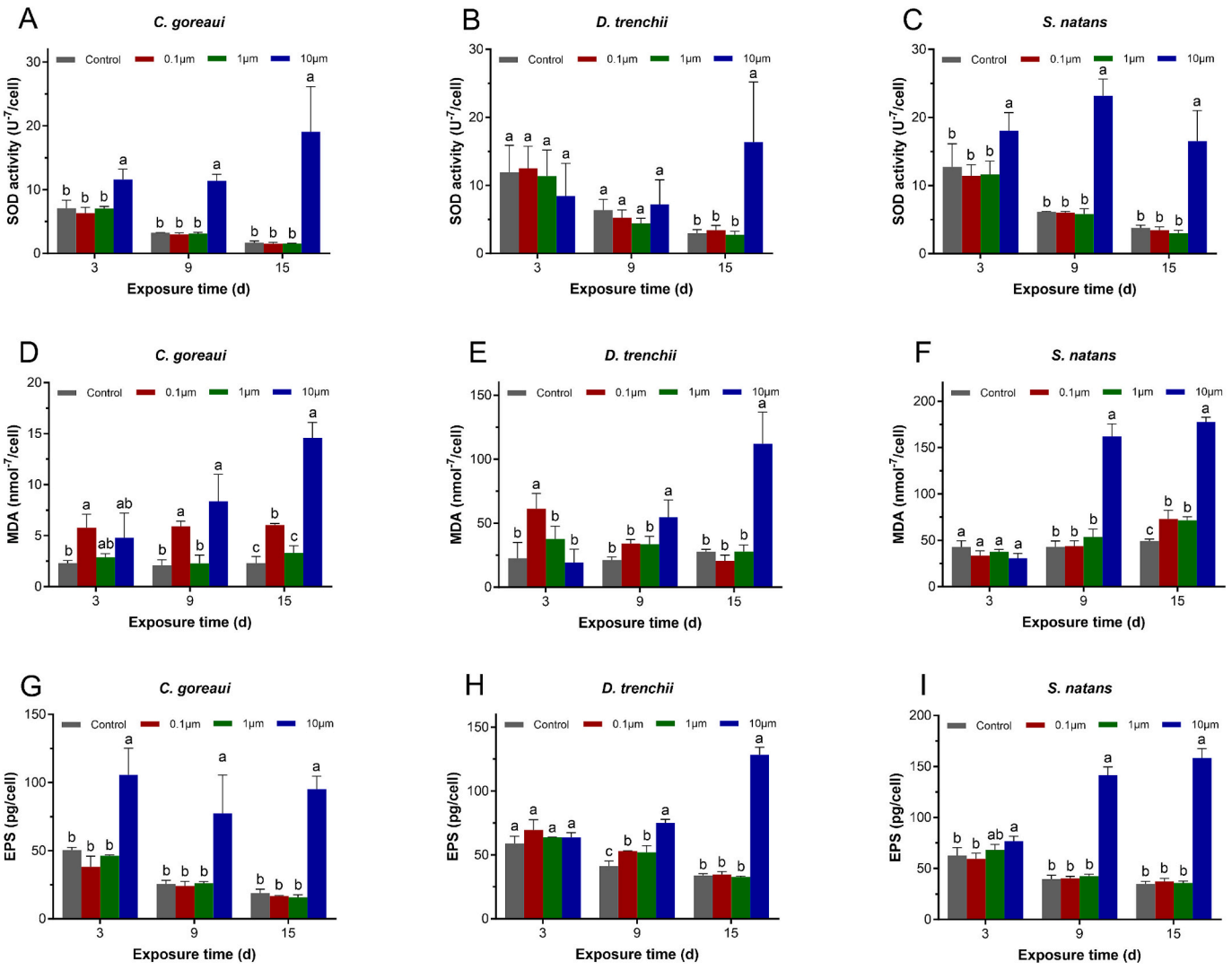

Fig. 3. Effects of PS-MPs of different particle sizes on the antioxidant system of *C. goreaui*, *D. trenchii*, and *S. natans*. (A–C) SOD activity: (A) *C. goreaui*, (B) *D. trenchii*, (C) *S. natans*. (D–F) MDA content: (D) *C. goreaui*, (E) *D. trenchii*, (F) *S. natans*. (G-I) EPS content: (G) *C. goreaui*, (H) *D. trenchii*, (I) *S. natans*. Bars represent the mean ± standard error (n = 3 biological replicates). Different letters (a, b, c, d) indicate statistically significant differences between groups ($p < 0.05$).

tricarboxylic acid (TCA) cycle pathways (Fig. 8D). The 1 μm group showed significant enrichment in endocytosis, histidine metabolism, cofactor biosynthesis, proteasome, pyrimidine metabolism, ribosome biogenesis in eukaryotes, and nitrogen metabolism (Fig. 8E). The 10 μm group was significantly enriched in starch and sucrose metabolism, fatty acid biosynthesis, and aminoacyl-tRNA biosynthesis (Fig. 8F). In addition, Gene Set Enrichment Analysis (GSEA) of the 10 μm group is presented in Fig. S4.

For *S. natans*, after exposure to PS-MPs, only the 1 μm group exhibited pathways enriched solely by upregulated DEGs (Fig. 8H). The 0.1 μm group contained only three downregulated pathways (Fig. 8G), while the 10 μm group included both exclusively downregulated pathways and pathways containing both up- and downregulated DEGs (Fig. 8I). In addition, DEGs in all three treatment groups were significantly enriched in carbohydrate metabolism pathways. The 1 μm group was significantly enriched in purine metabolism (Fig. 8H), while the 10 μm group showed pronounced enrichment in ribosome and photosynthesis pathways (Fig. 8I).

4. Discussion

4.1. Growth inhibition of *C. goreaui, D. trenchii, and S. natans* under PS-MP exposure

In recent years, with the severe degradation of coral reefs and the pivotal role of *Symbiodiniaceae* in reef ecosystems, increasing attention has been paid to the mechanisms underlying their responses to environmental stressors. As MP pollution intensifies, the toxic effects of MPs on *Symbiodiniaceae* have become a research focus. In this study, although the three algal species exhibited slightly different strategies in response to PS-MPs stress, they shared a consistent particle size–toxicity pattern—larger PS-MPs exerted stronger toxic effects. Consistent with the stronger inhibitory effects of large-sized PS-MPs (10 μm) on the growth of the three algal species in this study, Xiao et al. (2020) also reported that 5 μm PS-MPs (10 mg/L) exerted greater toxicity on *Euglena gracilis* growth compared with 0.1 μm particles. Similarly, Li et al. (2023) demonstrated that larger PS-MPs (0.3 and 0.5 μm) exhibited stronger toxicity to *Chlamydomonas reinhardtii* than smaller ones (50 nm). Wu et al. (2021) observed that 1 μm PS-MPs promoted the growth of *Microcystis aeruginosa* more strongly than 0.1 μm PS-MPs. Similarly, in this study, although the relatively environmentally sensitive *C. goreaui*

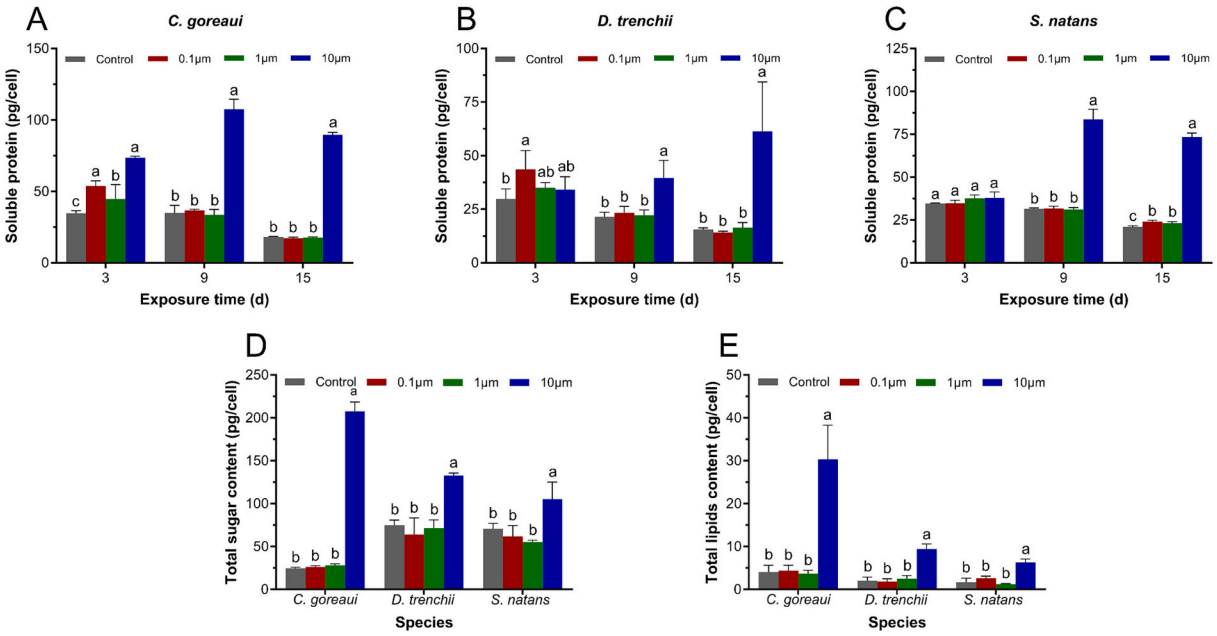

Fig. 4. Effects of PS-MPs of different particle sizes on intracellular metabolites in *C. goreaui*, *D. trenchii*, and *S. natans*. (A–C) Soluble protein content: (A) *C. goreaui*, (B) *D. trenchii*, (C) *S. natans*; (D) total carbohydrate content; (E) total lipid content.

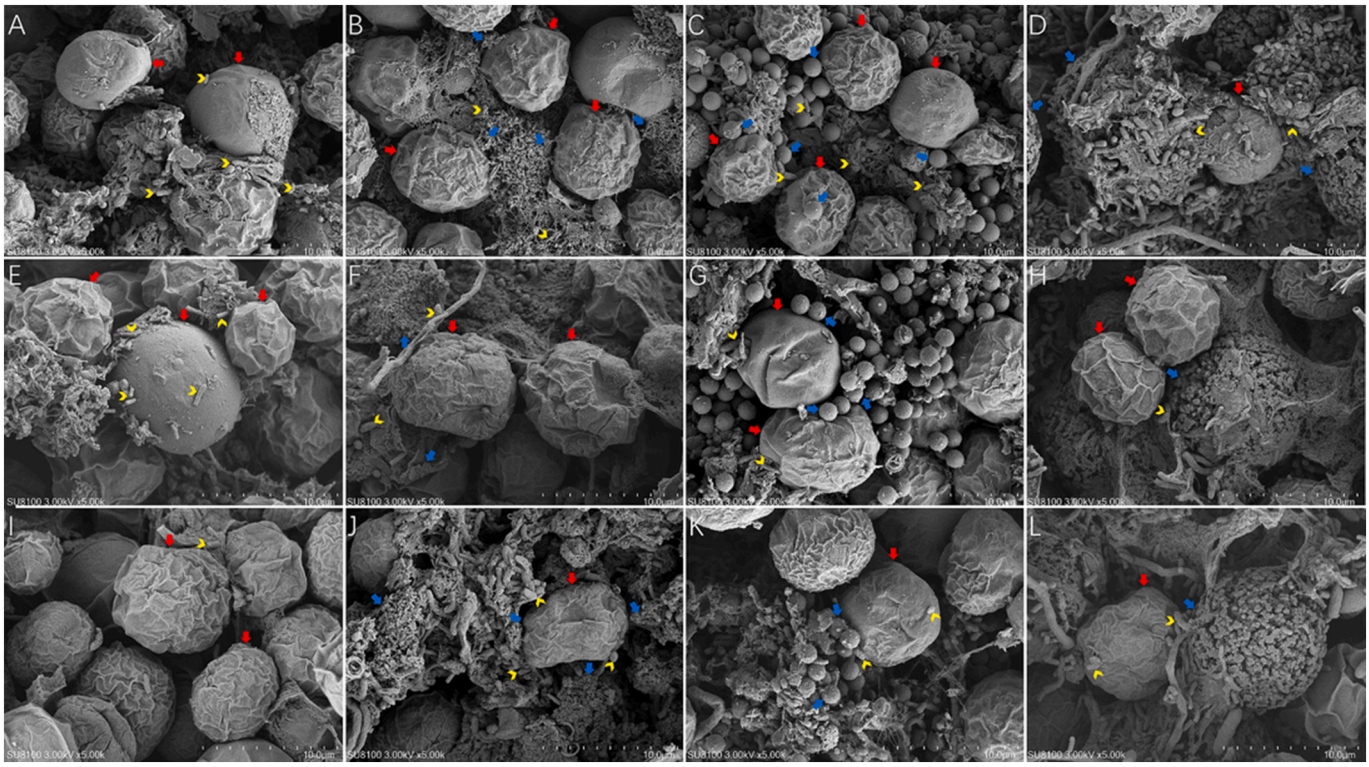

Fig. 5. Effects of PS-MPs of different sizes on the cell surfaces of *C. goreaui*, *D. trenchii*, and *S. natans*. (A–D) *C. goreaui*: (A) control; (B) 0.1 μm; (C) 1 μm; (D) 10 μm. (*E*-H) *D. trenchii*: (E) control; (F) 0.1 μm; (G) 1 μm; (H) 10 μm. (I–L) *S. natans*: (I) control; (J) 0.1 μm; (K) 1 μm; (L) 10 μm. Red arrows indicate algal cells, yellow arrows indicate symbiotic bacteria, and blue arrows indicate PS-MPs. (For interpretation of the references to color in this figure legend, the reader is referred to the web version of this article.)

and *S. natans* showed slight recovery in growth during the later stages, overall, 10 μm PS-MPs still exerted severe toxic effects on all three algal species. On the other hand, several studies have shown that smaller-sized MPs elicit stronger toxicity in microalgae (Chae et al., 2019; Li et al., 2020b), highlighting that algal responses to MP particle size are species-dependent. The interactions between MPs and microalgae, including shading effects and oxidative stress, are affected by factors such as increased negative charge and surface roughness, which can enhance growth inhibition (Xu et al., 2024). The observed loss of cytoplasmic ribosomal proteins in transcriptomic data could contribute to

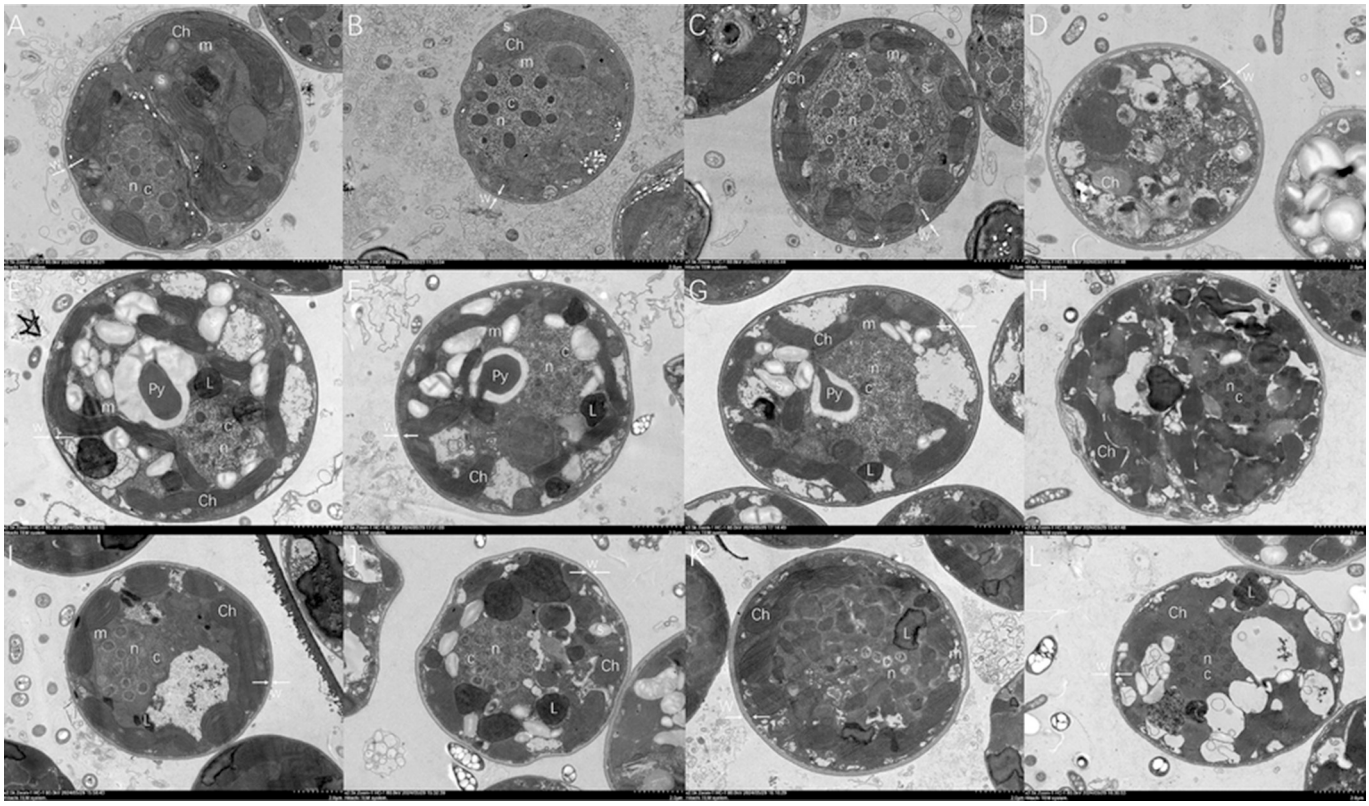

Fig. 6. Effects of PS-MPs of different sizes on the ultrastructure of *C. goreaui*, *D. trenchii*, and *S. natans* cells. (A–D) *C. goreaui*: (A) Control; (B) 0.1 μm; (C) 1 μm; (D) 10 μm. (E–H) *D. trenchii*: (E) Control; (F) 0.1 μm; (G) 1 μm; (H) 10 μm. (I–L) *S. natans*: (I) Control; (J) 0.1 μm; (K) 1 μm; (L) 10 μm. Abbreviations: n, nucleus; c, chromosome; Ch, chloroplast; Py, pyrenoid; m, mitochondrion; s, starch; L, lipids; w, cell wall (paired arrows indicate cell wall thickness); v, vesicle.

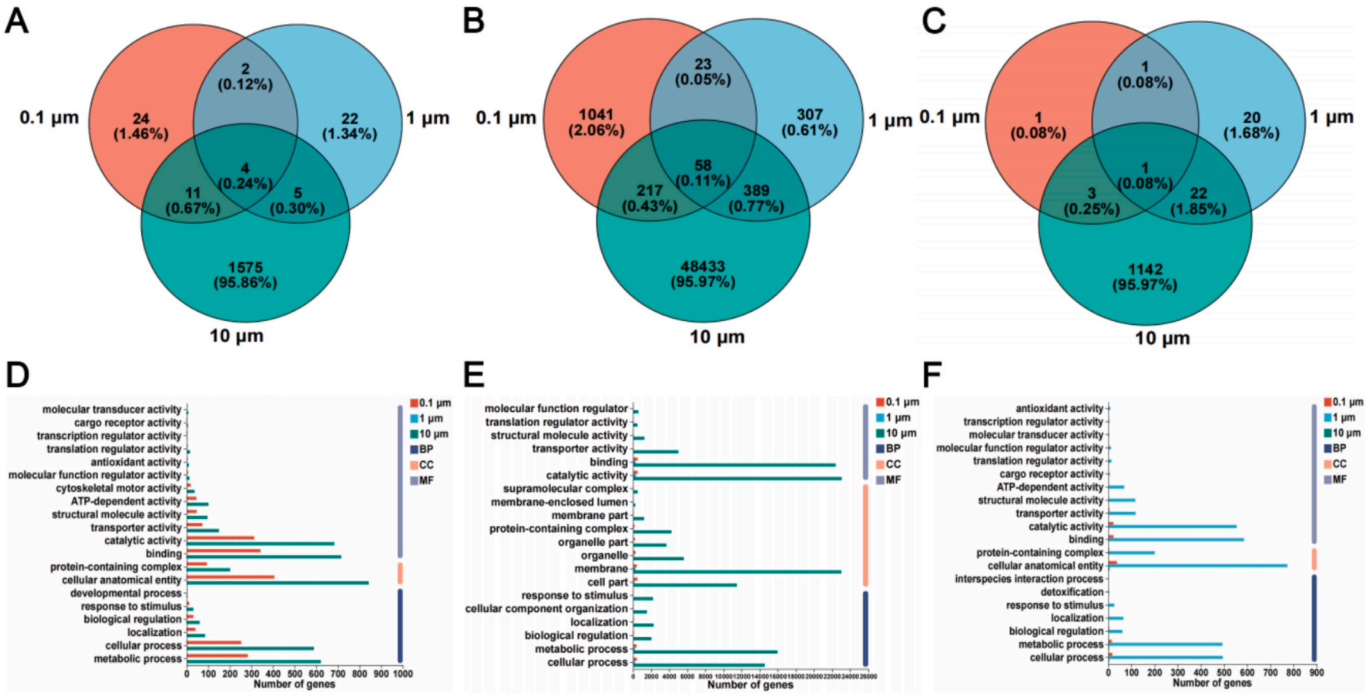

Fig. 7. Venn diagrams and GO functional annotation of DEGs in *C. goreaui*, *D. trenchii*, and *S. natans* following exposure to PS-MPs. (A–C) Venn diagrams of DEGs: (A) *C. goreaui*, (B) *D. trenchii*, (C) *S. natans*. (D–F) GO functional annotation of DEGs: (D) *C. goreaui*, (E) *D. trenchii*, (F) *S. natans*.

reduced growth rates (Szakonyi and Byrne, 2011). Downregulation of multiple ribosomal protein-encoding genes within the ribosome pathway is likely to suppress cellular growth (Fig. 9).

In addition, Su et al. (2020) found that 1 μm PS-MPs (5 mg/L) reduced *C. goreaui* cell size on days 6–7. Similarly, in this study, *C. goreaui* cells exposed to 1 μm PS-MPs for 9 days exhibited a significant

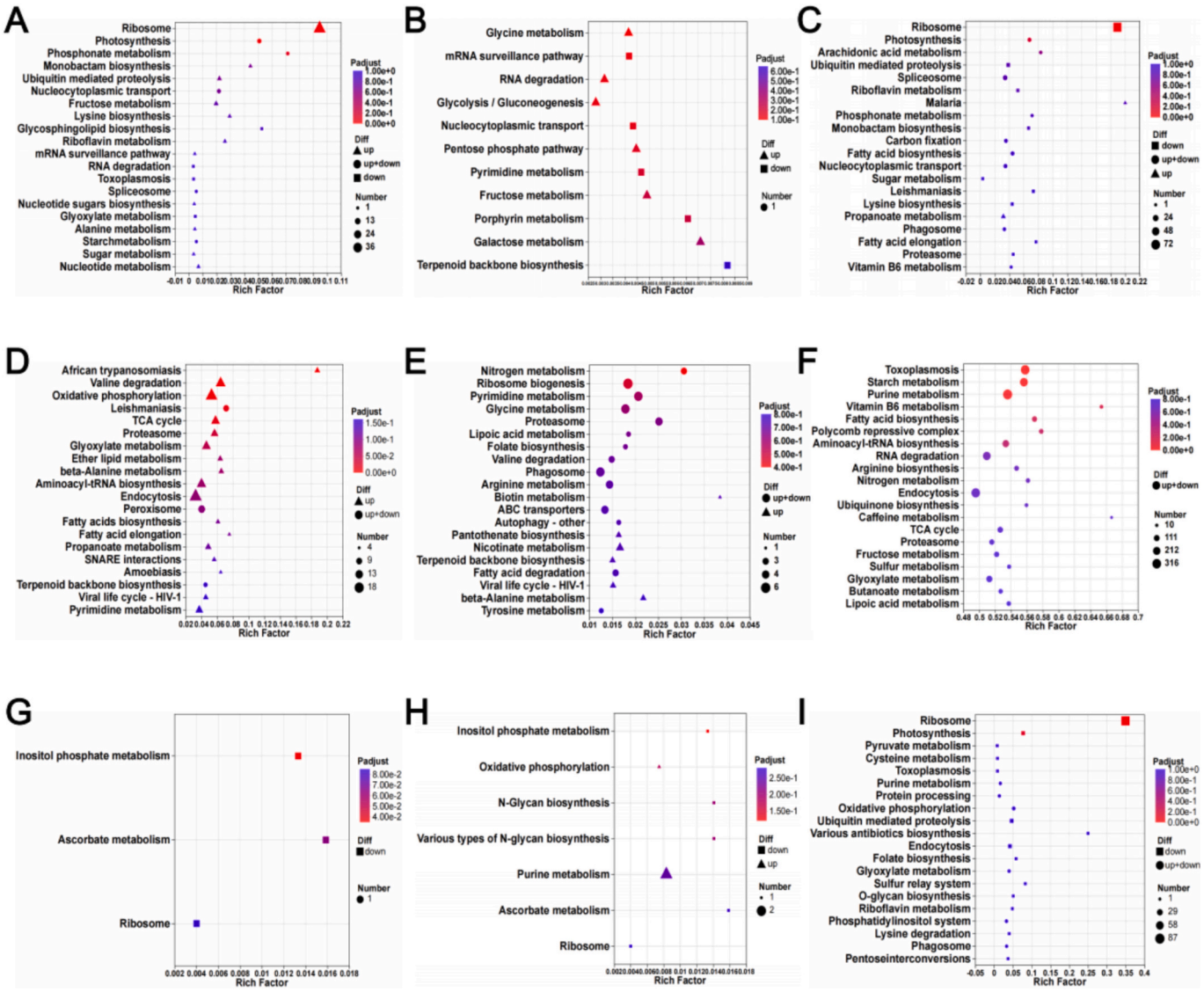

Fig. 8. KEGG pathway enrichment analysis of *C. goreaui*, *D. trenchii*, and *S. natans* in response to PS-MP exposure. (A–C) Bubble plots showing KEGG pathway enrichment in *C. goreaui*: (A) 0.1 μm vs. Control; (B) 1 μm vs. Control; (C) 10 μm vs. Control. (D–F) Bubble plots showing KEGG pathway enrichment in *D. trenchii*: (D) 0.1 μm vs. Control; (E) 1 μm vs. Control; (F) 10 μm vs. Control. (G–I) Bubble plots showing KEGG pathway enrichment in *S. natans*: (G) 0.1 μm vs. Control; (H) 1 μm vs. Control; (I) 10 μm vs. Control.

reduction in cell size. In contrast, Hazeem et al. (2020) reported a slight increase in *Chlorella vulgaris* cell size after exposure to 20 nm PS particles, while Chae et al. (2019) showed that 180–212 μm PS-MPs at 150 mg/L enlarged *Dunaliella salina* cells. Cheng et al. (2024) further demonstrated that MPs of PP, PE, and PET (100 mg/L) increased *C. vulgaris* cell size. Long et al. (2017) proposed that MP exposure may increase algal cell volume by promoting growth while suppressing division, which aligns with the present findings. In our study, exposure to 10 μm PS-MPs significantly enlarged cells of *C. goreaui*, *D. trenchii*, and *S. natans*. The concomitant decrease in cell density with cell volume expansion is consistent with observations by Gao et al. (2024). The pronounced cell enlargement induced by 10 μm PS-MPs is likely attributable to inhibited cell division, in agreement with previous studies showing that MPs increase cell diameter and membrane permeability, thereby disturbing division and material exchange and ultimately suppressing proliferation (Ye et al., 2023; Cheng et al., 2024).

Cell enlargement may also result from reduced light penetration under 10 μm PS-MP exposure, which could drive algae to expand their light-harvesting surface area for enhanced photon capture. Moreover, the rough surfaces of 10 μm PS-MPs may induce physical damage, triggering osmotic swelling under hypotonic conditions (Li et al., 2020a; Jiang et al., 2025). TEM observations, including nuclear disintegration, cytoplasmic vacuolization, and increased membrane permeability, further corroborate impaired algal growth and development. To maintain osmotic balance, algal cells increase water uptake into vacuoles, which in turn leads to vacuolar swelling (Xiao et al., 2020; Jiang et al., 2025).

4.2. Photosynthetic inhibition of *C. goreaui*, *D. trenchii*, and *S. natans* under PS-MPs exposure

Excessive MPs can induce shading effects through cell aggregation, thereby reducing light availability and altering the transcriptional activity of photosynthesis-related genes. Previous studies have shown that 1 μm PS-MPs can form dense EPS-MP complexes on the surface of *Chlorella pyrenoidosa*, significantly impairing its light-harvesting capacity (Cao et al., 2022). Under light-limited conditions, algal cells can upregulate chlorophyll biosynthesis to enhance photosynthetic

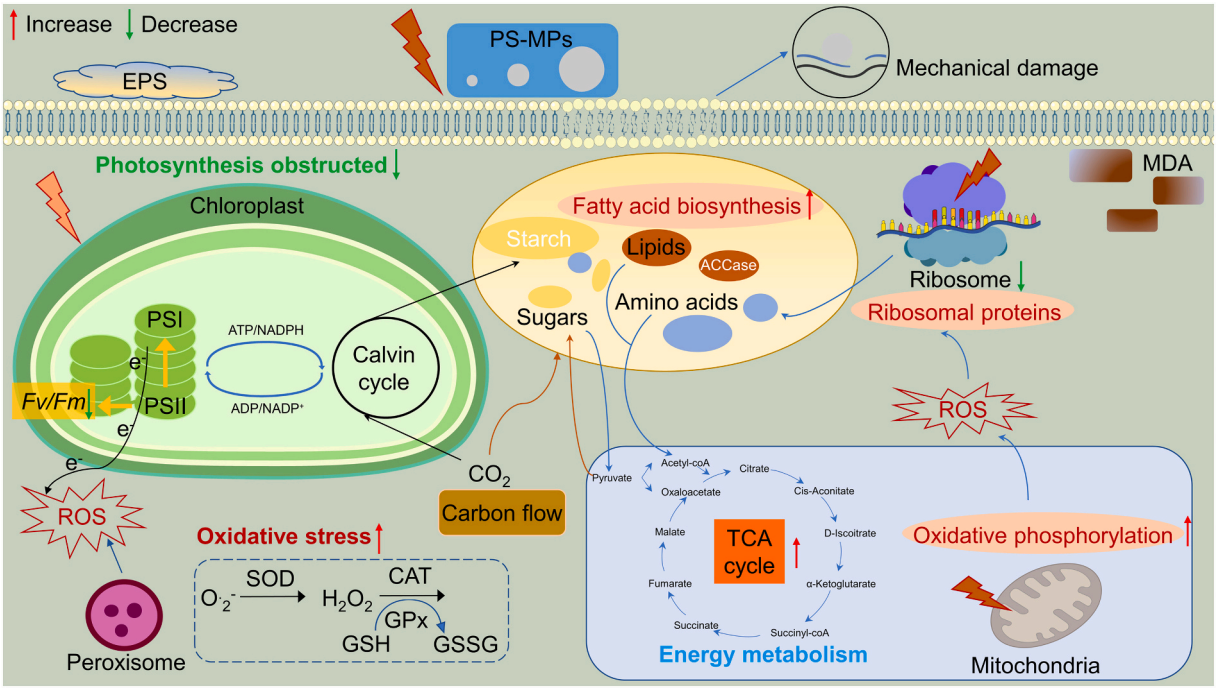

Fig. 9. Schematic diagram of the toxicity mechanism of PS-MPs exposure to *Symbiodiniaceae*. ACCase: acetyl-CoA carboxylase; CAT: catalase; GPx: glutathione peroxidase; GSH: glutathione, reduced form; GSSG: glutathione disulfide.

efficiency and maintain photostability (Falkowski and Owens, 1980). In corals, symbiotic brown algae transform from a single-layer arrangement to a multilayer structure under low-temperature, low-light winter conditions to improve light capture efficiency, whereas during high-temperature, high-light summer conditions, their cell density and photosynthetic pigment content decrease markedly (Venn et al., 2008). These seasonal adaptations indicate that algal symbionts can maintain photosynthetic homeostasis by modulating pigment composition.

In this study, exposure to 10 μm PS-MPs significantly reduced Fv/Fm in all three algal species, likely due to the shading effect of microplastics impairing photosynthetic activity. Previous studies have suggested that light obstruction is the primary toxic mechanism for larger microplastic particles (Liu et al., 2019; Li et al., 2023). As particulate pollutants, 10 μm PS-MPs may hinder light transmission around microalgal cells, reducing light availability and consequently limiting photosynthetic autotrophic growth (Huang et al., 2024). SEM and TEM images confirmed that after PS-MPs exposure, all three algae exhibited extensive EPS production and severe cellular damage, including cell shrinkage and chloroplast disintegration, leading to diminished photosynthetic capacity. However, the heterogeneous aggregation between microalgae and PS-MPs may represent one of the mechanisms by which microalgae mitigate the toxicity of PS microplastics in aquatic environments (Su et al., 2022). As the number of aggregates increases, PS-MPs are more likely to settle to the bottom, potentially providing a relatively favorable growth environment for the algae. This also explains the gradually recovering trend in photosynthetic activity observed in the three algal species during the later stages of exposure. Changes in Chl-a content may reflect the algal response to reduced light availability, a phenomenon previously observed in similar studies (Liang et al., 2025). Furthermore, the subsequent decline in chlorophyll content may be associated with intracellular ROS accumulation, which can damage cellular structures and inhibit chlorophyll biosynthesis (Wu et al., 2019; Jiang et al., 2025). Transcriptomic analysis also revealed that pathways related to pigment biosynthesis and photosynthetic performance were substantially affected.

It should be noted that while the flasks were manually agitated daily to mitigate sedimentation, the actual exposure dynamics could be influenced by particle aggregation and interactions with EPS over the 18-day period. Microplastics, particularly the 10 μm PS-MPs, may undergo settle-down or hetero-aggregation with algal cells and their secreted EPS, leading to temporal variations in effective exposure concentrations and particle distribution. Such dynamics might have contributed to the observed 'recovery' trends in the later stages by reducing the suspended concentration of stressors, a common limitation in static exposure experiments that warrants further investigation using semi-continuous or flow-through systems.

4.3. *Oxidative damage and metabolic dysfunction in C. goreaui, D. trenchii, and S. natans following PS-MPs exposure*

Pollutants often stimulate the production of antioxidant enzymes in microalgal cells. SOD plays a critical role in scavenging ROS induced by oxidative stress and mitigating the potential toxicity of pollutants to organisms (Chae et al., 2019). The significant increase in SOD levels observed in the 10 μm PS-MPs groups across the three algal species indicates that large-sized PS-MPs can induce oxidative stress and activate their antioxidant defense systems. Oxidative stress is a crucial response of microalgae to environmental stressors, and previous studies have extensively investigated the toxicity of microplastics from the perspective of oxidative stress (Li et al., 2024). To counteract ROS generated under oxidative stress, microalgae upregulate antioxidant enzymes to protect cells from damage (Zhu et al., 2023). However, excessive ROS accumulation can promote lipid peroxidation of cellular membranes. MDA, a major end product of lipid peroxidation, serves as a biomarker of oxidative stress in organisms (Khoubnasabjafari et al., 2015). In this study, exposure to 0.1 μm, 1 μm, and 10 μm PS-MPs all led to increased MDA levels, indicating varying degrees of oxidative damage in the three algal species. Moreover, lipid peroxidation was particularly pronounced in the 10 μm PS-MPs treatment, with MDA content continuing to rise over time, suggesting that the antioxidant defense system was insufficient to eliminate excessive ROS in the algal cells.

Under stress conditions, such as when MPs adhere to the cell wall, microalgae can be stimulated to produce large amounts of EPS (Hazeem et al., 2020). EPS are complex high-molecular-weight polymers secreted

by microorganisms, primarily composed of proteins and polysaccharides (Zhao et al., 2024). The significant increase in EPS content observed in three algal species upon exposure to 10 μm PS-MPs indicates that PS-MPs can stimulate microalgae to enhance EPS production (Mao et al., 2018; Su et al., 2022). EPS can facilitate heteroaggregation between microalgae and microplastics, as well as homoaggregation among algal cells (Long et al., 2017). Moreover, EPS may act as a biological barrier, maintaining cell integrity and limiting microplastic internalization, thereby mitigating their toxicity (Gao et al., 2018). However, despite the elevated levels of EPS and antioxidant enzymes, the significant decreases in *Fv/Fm* values and cell density suggest that these defense mechanisms are insufficient to fully counteract the damage caused by high concentrations of 10 μm PS-MPs (Huang et al., 2024).

Proteins, carbohydrates, and lipids are essential intracellular components in microalgae, involved in energy supply, structural maintenance, and various metabolic processes (Jiang et al., 2024). Li et al. (2020a) reported that exposure to PS microplastics increased the soluble protein content in *C. reinhardtii*, likely due to physical damage to the algal surface that alters cellular osmotic pressure. The accumulation of soluble proteins may enhance water retention, thereby protecting vital cellular components and biomembranes (Guzman-Murillo et al., 2007). Consistently, our results indicate that long-term exposure to PS-MPs of all three particle sizes promoted an increase in soluble protein content in *C. goreaui*, *D. trenchii*, and *S. natans*. The increased starch content observed in TEM analysis, together with the differential expression of metabolic functions in the transcriptome, provides strong evidence supporting this mechanism.

The increase in total carbohydrate and lipid content observed in the 10 μm group of the three algal species may represent an energy storage strategy employed by algal cells to resist toxic stress. Previous studies have shown that oxidative stress can lead to increased starch accumulation in algae (Hazeem et al., 2020), and microalgae tend to synthesize more lipids under environmental stress to sustain survival (Sun et al., 2023; Xu et al., 2024). Cheng et al. (2024) reported that PET and PP significantly induced an increase in total carbohydrate content in *C. vulgaris*. Similarly, Ansari et al. (2021) found that high-density polyethylene (HDPE) at concentrations of 5–150 mg/L increased the carbohydrate content of *Acutodesmus obliquus* by 0.65–7.5%. Lagarde et al. (2016) observed that *C. reinhardtii* exposed to PP and HDPE for over 70 days exhibited significant overexpression of genes related to carbohydrate synthesis, indicating that microplastics can promote excessive intracellular carbohydrate accumulation. These findings suggest that exposure to 10 μm PS-MPs may impose survival pressure on algal cells (Zhu et al., 2023), prompting them to enhance lipid synthesis as a means of energy storage and stress alleviation (Zhang et al., 2018). Reduced photosynthetic activity redirects carbon flux toward storage molecules such as starch and neutral lipids, rather than supporting cell division or growth (Li et al., 2011). This phenomenon is generally associated with adjustments in cellular energy allocation (Burlacot et al., 2022), which enable algae to survive under stress and provide energy and carbon reserves for subsequent recovery and regeneration (Hildebrand et al., 2013; Adesanya et al., 2014).

Although the integrated physiological and transcriptomic data presented here provide a comprehensive overview of the PS-MP impact, it is important to clarify that most observed responses—such as oxidative stress, photosynthetic impairment, and gene expression changes—are based on strong correlations. While these findings strongly suggest a size-dependent toxicity mechanism, the direct causal linkage between specific transcriptomic shifts and physiological failure remains to be definitively proven through functional validation, such as the use of targeted inhibitors or gene knockout studies. Thus, the proposed mechanisms should be interpreted as a potential toxicity pathway that requires further experimental verification to isolate individual causal drivers.

4.4. Ecological implications of size-dependent PS-MP toxicity for *Symbiodiniaceae*

Although this study focuses on cellular, physiological, and transcriptomic responses of *Symbiodiniaceae* to polystyrene microplastics, the observed size-dependent toxicity has important ecological implications for coral reef ecosystems. As the primary photosynthetic partners of reef-building corals, *Symbiodiniaceae* underpin coral energy acquisition, stress tolerance, and long-term reef accretion. Therefore, disturbances at the algal level can propagate across biological scales, ultimately influencing coral health and ecosystem resilience. Our results demonstrate that larger-sized PS-MPs (10 μm) induced the most pronounced adverse effects on *Symbiodiniaceae*, including growth inhibition, photosynthetic suppression, oxidative damage, and extensive metabolic reprogramming. These responses are ecologically relevant because free-living *Symbiodiniaceae* populations constitute the main environmental reservoir for symbiont acquisition, particularly for coral species that rely on horizontal transmission (Baird et al., 2009; Ali et al., 2019). Impairment of algal growth and photosynthetic capacity in the surrounding environment may reduce symbiont availability and quality, thereby constraining coral recruitment, symbiosis establishment, and post-disturbance recovery.

Photosynthetic inhibition observed under 10 μm PS-MP exposure is especially critical from an ecological perspective. Reduced *Fv/Fm* values, chloroplast damage, and downregulation of photosynthesis-related genes collectively indicate compromised photochemical efficiency and carbon fixation. In coral-algal symbioses, such reductions directly translate into decreased translocation of photosynthates to the host, weakening coral energy budgets and increasing susceptibility to additional stressors such as thermal anomalies and nutrient imbalance (Putnam et al., 2017). Even in free-living stages, reduced photosynthetic performance may limit algal persistence in oligotrophic reef waters, thereby indirectly affecting symbiont supply dynamics.

Oxidative stress represents another key ecological link between microplastic exposure and coral reef vulnerability. Elevated SOD activity and sustained MDA accumulation under 10 μm PS-MPs indicate that *Symbiodiniaceae* experience chronic oxidative pressure that exceeds their antioxidant buffering capacity. Oxidative stress has long been recognized as a central mechanism driving coral bleaching, as excessive reactive oxygen species can disrupt cellular homeostasis and trigger symbiosis breakdown. Although bleaching was not directly assessed in this study, the observed oxidative responses at the algal level suggest that microplastic exposure may lower the oxidative stress threshold of *Symbiodiniaceae*, rendering coral–algal associations more fragile under co-occurring environmental stressors.

Furthermore, the marked increase in EPS production and heteroaggregation between *Symbiodiniaceae* and PS-MPs has dual ecological implications. On the one hand, EPS secretion may represent an adaptive defense strategy that limits direct particle contact and internalization. On the other hand, excessive EPS production can promote particle aggregation, alter light microenvironments, and increase sedimentation rates. In reef systems, such aggregation processes may modify particle residence times and spatial distribution, potentially enhancing microplastic accumulation in benthic habitats where many coral recruits and symbionts reside.

4.5. Implications for coral health and reef ecosystem resilience

Beyond immediate algal-level effects, the size-dependent toxicity of PS-MPs observed in this study has broader implications for coral health and reef ecosystem resilience. The pronounced toxicity of 10 μm PS-MPs, despite their larger size, highlights the importance of physical interactions, shading effects, and surface-mediated damage in particle-rich reef environments. In natural settings, reef waters frequently experience elevated turbidity due to sediment resuspension, storm events, and anthropogenic disturbances, conditions under which larger

microplastic particles may exert disproportionate ecological impacts.

The observed metabolic reprogramming toward carbohydrate and lipid accumulation under severe PS-MP stress further suggests a shift in carbon allocation from growth and division toward survival and energy storage. While such metabolic adjustments may enhance short-term stress tolerance of *Symbiodiniaceae*, they may also reduce the efficiency of carbon translocation to coral hosts once symbiosis is established. Over time, this could weaken coral energy budgets, impair calcification, and slow reef accretion processes.

Species-specific responses observed among *C. goreaui*, *D. trenchii*, and *S. natans* provide additional ecological insight. The relatively higher sensitivity of *C. goreaui*—a dominant and widely distributed coral symbiont—suggests that microplastic pollution may selectively disadvantage symbionts that support many reef-building corals. In contrast, the greater metabolic plasticity observed in *D. trenchii* may partially explain its association with stress-tolerant coral hosts. Such differential sensitivities could contribute to shifts in symbiont community composition under chronic microplastic exposure, with unknown long-term consequences for coral performance and reef biodiversity.

Taken together, these findings indicate that microplastic pollution, particularly involving larger microplastic particles, should be considered an emerging factor influencing coral–algal symbiosis stability. By impairing *Symbiodiniaceae* physiology, altering stress tolerance, and reshaping symbiont availability, microplastics may act synergistically with climate-driven stressors to accelerate reef degradation. Understanding these algal-mediated pathways is therefore essential for accurately assessing the ecological risks of microplastic pollution in coral reef ecosystems.

5. Conclusion

Our study reveals that the toxicity of polystyrene microplastics (PS-MPs) on symbiotic *Symbiodiniaceae* is strongly dependent on both particle size and species identity. Among the tested sizes, 10 μm PS-MPs elicited the most severe adverse effects, including inhibition of cell proliferation and photosynthesis, cell enlargement, and enhanced accumulation of carbohydrates and lipids. Morphological and transcriptomic analyses indicated that these effects are primarily mediated through membrane and chloroplast disruption, extracellular polymeric substance (EPS) formation, and downregulation of ribosomal and photosynthetic genes. Importantly, different species exhibited distinct detoxification strategies: *D. trenchii* alleviated 0.1 μm PS-MPs stress by upregulating oxidative phosphorylation and the TCA cycle, whereas *S. natans* countered 1 μm PS-MPs toxicity via activation of purine metabolism and oxidative phosphorylation. In response to 10 μm PS-MPs, all species enhanced fatty acid biosynthesis and antioxidant defenses, partially mitigating stress. Collectively, these findings provide mechanistic insights into the size- and species-specific toxicity of PS-MPs on coral-algal symbiosis and underscore the urgent need for effective mitigation strategies to preserve coral reef ecosystem resilience.

CRediT authorship contribution statement

Jiayuan Liang: Writing – review & editing, Writing – original draft, Validation, Resources, Project administration, Funding acquisition, Formal analysis, Data curation, Conceptualization. **Yating Yang:** Writing – review & editing, Writing – original draft, Visualization, Methodology. **Tianyi Niu:** Writing – review & editing. **Zhicong Li:** Writing – review & editing. **Zhuqing Liang:** Writing – review & editing. **Mingyao Lu:** Writing – review & editing. **Li Zhang:** Writing – review & editing. **Yihe Feng:** Writing – review & editing. **Sanqiang Gong:** Validation, Software. **Kefu Yu:** Supervision, Project administration, Funding acquisition.

Declaration of competing interest

The authors declare that they have no known competing financial interests or personal relationships that could have appeared to influence the work reported in this paper.

Acknowledgements

This work was supported by the National Natural Science Foundation of China (42030502 and 42090041), the Self-Topic Project of Guangxi Laboratory on the Study of Coral Reefs in the South China Sea (GXLSCRSCS2023101), and the Science and Technology Project of Guangxi (Nos. AD17129063 and AA17204074).

Appendix A. Supplementary data

Supplementary data to this article can be found online at https://doi.org/10.1016/j.marpolbul.2026.119697.

Data availability

The data generated as part of this study are available upon request. The raw sequence data (a total of 36 RNA sequencing libraries) produced in this study were deposited in the Sequence Read Archive (PRJNA1242092) of the NCBI (https://www.ncbi.nlm.nih.gov).

References

Abinandan, S., Praveen, K., Venkateswarlu, K., Megharaj, M., 2023. Microalgae-microplastics interactions at environmentally relevant concentrations: implications toward ecology, bioeconomy, and UN SDGs. Water Res. 247, 120778. https://doi.org/10.1016/j.watres.2023.120778.

Adesanya, V.O., Davey, M.P., Scott, S.A., Smith, A.G., 2014. Kinetic modelling of growth and storage molecule production in microalgae under mixotrophic and autotrophic conditions. Bioresour. Technol. 157, 293–304. https://doi.org/10.1016/j.biortech.2014.01.032.

Ali, A., Kriefall, N.G., Emery, L.E., Kenkel, C.D., Matz, M.V., Davies, S.W., 2019. Recruit symbiosis establishment and Symbiodiniaceae composition influenced by adult corals and reef sediment. Coral Reefs 38 (3), 405–415. https://doi.org/10.1007/s00338-019-01790-z.

Ansari, F.A., Ratha, S.K., Renuka, N., Ramanna, L., Gupta, S.K., Rawat, I., Bux, F., 2021. Effect of microplastics on growth and biochemical composition of microalga Acutodesmus obliquus. Algal Res. Biomass Biofuels Bioprod. 56, 102296. https://doi.org/10.1016/j.algal.2021.102296.

Baird, A.H., Guest, J.R., Willis, B.L., 2009. Systematic and biogeographical patterns in the reproductive biology of Scleractinian corals. Annu. Rev. Ecol. Evol. Syst. 40, 551–571. https://doi.org/10.1146/annurev.ecolsys.110308.120220.

Berry, K.L.E., Epstein, H.E., Lewis, P.J., Hall, N.M., Negri, A.P., 2019. Microplastic contamination has limited effects on coral fertilisation and larvae. Diversity 11 (12), 228. https://doi.org/10.3390/d11120228.

Burlacot, A., Dao, O., Auroy, P., Cuiné, S., Li-Beisson, Y., Peltier, G., 2022. Alternative photosynthesis pathways drive the algal CO2-concentrating mechanism. Nature 605 (7909), 366–371. https://doi.org/10.1038/s41586-022-04662-9.

Cao, Q., Sun, W., Yang, T., Zhu, Z., Jiang, Y., Hu, W., Wei, W., Zhang, Y., Yang, H., 2022. The toxic effects of polystyrene microplastics on freshwater algae Chlorella pyrenoidosa depends on the different size of polystyrene microplastics. Chemosphere 308, 136135.

Chae, Y., Kim, D., An, Y.-J., 2019. Effects of micro-sized polyethylene spheres on the marine microalga Dunaliella salina: focusing on the algal cell to plastic particle size ratio. Aquat. Toxicol. 216, 105296. https://doi.org/10.1016/j.aquatox.2019.105296.

Chen, B., Yu, K., Qin, Z., Liang, J., Wang, G., Huang, X., Wu, Q., Jiang, L., 2020. Dispersal, genetic variation, and symbiont interaction network of heat-tolerant endosymbiont Durusdinium trenchii: insights into the adaptive potential of coral to climate change. Sci. Total Environ. 723, 138026. https://doi.org/10.1016/j.scitotenv.2020.138026.

Cheng, S., Yoshikawa, K., Cross, J.S., 2024. Influence of synthetic and natural microfibers on the growth, substance exchange, energy accumulation, and oxidative stress of field-collected microalgae compared with microplastic fragment. Sci. Total Environ. 908, 167936. https://doi.org/10.1016/j.scitotenv.2023.167936.

Cole, M., Lindeque, P.K., Fileman, E., Clark, J., Lewis, C., Halsband, C., Galloway, T.S., 2016. Microplastics alter the properties and sinking rates of zooplankton faecal pellets. Environ. Sci. Technol. 50 (6), 3239–3246. https://doi.org/10.1021/acs.est.5b05905.

Collignon, A., Hecq, J.-H., Galgani, F., Collard, F., Goffart, A., 2014. Annual variation in neustonic micro- and meso-plastic particles and zooplankton in the Bay of Calvi

(Mediterranean-Corsica). Mar. Pollut. Bull. 79 (1–2), 293–298. https://doi.org/10.1016/j.marpolbul.2013.11.023.
Covernton, G.A., Pearce, C.M., Gurney-Smith, H.J., Chastain, S.G., Ross, P.S., Dower, J. F., Dudas, S.E., 2019. Size and shape matter: a preliminary analysis of microplastic sampling technique in seawater studies with implications for ecological risk assessment. Sci. Total Environ. 667, 124–132. https://doi.org/10.1016/j.scitotenv.2019.02.346.
Davy, S.K., Allemand, D., Weis, V.M., 2012. Cell biology of cnidarian-dinoflagellate symbiosis. Microbiol. Mol. Biol. Rev. 76 (2), 229–261. https://doi.org/10.1128/mmbr.05014-11.
Falkowski, P.G., Owens, T.G., 1980. Light-shade adaptation: two strategies in marine phytoplankton. Plant Physiol. 66 (4), 592–595. https://doi.org/10.1104/pp.66.4.592.
Gao, X., Zhou, K., Zhang, L., Yang, K., Lin, D., 2018. Distinct effects of soluble and bound exopolymeric substances on algal bioaccumulation and toxicity of anatase and rutile TiO2 nanoparticles. Environ. Sci. Nano 5 (3), 720–729. https://doi.org/10.1039/c7en01176h.
Gao, G., Zhao, X., Jin, P., Gao, K., Beardall, J., 2021. Current understanding and challenges for aquatic primary producers in a world with rising micro- and nano-plastic levels. J. Hazard. Mater. 406, 124685. https://doi.org/10.1016/j.jhazmat.2020.124685.
Gao, B., Wang, Y., Long, C., Long, L., Yang, F., 2024. Microplastics inhibit the growth of endosymbiotic Symbiodinium tridacnidorum by altering photosynthesis and bacterial community. Environ. Pollut. 346, 123603. https://doi.org/10.1016/j.envpol.2024.123603.
Guzman-Murillo, M.A., Lopez-Bolanos, C.C., Ledesma-Verdejo, T., Roldan-Libenson, G., Cadena-Roa, M.A., Ascencio, F., 2007. Effects of fertilizer-based culture media on the production of exocellular polysaccharides and cellular superoxide dismutase by Phaeodactylum tricornutum (Bohlin). J. Appl. Phycol. 19 (1), 33–41. https://doi.org/10.1007/s10811-006-9108-9.
Hansen, G., Daugbjerg, N., 2009. Symbiodinium natans sp. nov.: a “free-living” dinoflagellate from Tenerife (Northeast-Atlantic Ocean) 1. J. Phycol. 45 (1), 251–263. https://doi.org/10.1111/j.1529-8817.2008.00621.x.
Hazeem, L.J., Yesilay, G., Bououdina, M., Perna, S., Cetin, D., Suludere, Z., Barras, A., Boukherroub, R., 2020. Investigation of the toxic effects of different polystyrene micro-and nanoplastics on microalgae Chlorella vulgaris by analysis of cell viability, pigment content, oxidative stress and ultrastructural changes. Mar. Pollut. Bull. 156, 111278. https://doi.org/10.1016/j.marpolbul.2020.111278.
Hildebrand, M., Abbriano, R.M., Polle, J.E., Traller, J.C., Trentacoste, E.M., Smith, S.R., Davis, A.K., 2013. Metabolic and cellular organization in evolutionarily diverse microalgae as related to biofuels production. Curr. Opin. Chem. Biol. 17 (3), 506–514. https://doi.org/10.1016/j.cbpa.2013.02.027.
Huang, J., Wang, H., Xue, X., Zhang, R., 2024. Impacts of microplastic and seawater acidification on unicellular red algae: growth response, photosynthesis, antioxidant enzymes, and extracellular polymer substances. Aquat. Toxicol. 272, 106960. https://doi.org/10.1016/j.aquatox.2024.106960.
Jiang, J., Cai, X., Ren, H., Cao, G., Meng, J., Xing, D., Vollertsen, J., Liu, B., 2024. Effects of polyethylene terephthalate microplastics on cell growth, intracellular products and oxidative stress of Scenedesmus sp. Chemosphere 348, 140760. https://doi.org/10.1016/j.chemosphere.2023.140760.
Jiang, S., Lu, H., Xie, Y., Zhou, T., Dai, Z., Sun, R., He, L., Li, C., 2025. Toxicity of microplastics and nano-plastics to coral-symbiotic alga (Dinophyceae Symbiodinium): evidence from alga physiology, ultrastructure, OJIP kinetics and multi-omics. Water Res. 273, 123002. https://doi.org/10.1016/j.watres.2024.123002.
Khoubnasabjafari, M., Ansarin, K., Jouyban, A., 2015. Reliability of malondialdehyde as a biomarker of oxidative stress in psychological disorders. BioImpacts 5 (3), 123–127. https://doi.org/10.15171/bi.2015.20.
Lagarde, F., Olivier, O., Zanella, M., Daniel, P., Hiard, S., Caruso, A., 2016. Microplastic interactions with freshwater microalgae: hetero-aggregation and changes in plastic density appear strongly dependent on polymer type. Environ. Pollut. 215, 331–339. https://doi.org/10.1016/j.envpol.2016.05.006.
LaJeunesse, T.C., Parkinson, J.E., Gabrielson, P.W., Jeong, H.J., Reimer, J.D., Voolstra, C.R., Santos, S.R., 2018. Systematic revision of Symbiodiniaceae highlights the antiquity and diversity of coral endosymbionts. Curr. Biol. 28 (16), 2570–2580. https://doi.org/10.1016/j.cub.2018.07.008.
Lamb, J.B., Willis, B.L., Fiorenza, E.A., Couch, C.S., Howard, R., Rader, D.N., True, J.D., Kelly, L.A., Ahmad, A., Jompa, J., Harvell, C.D., 2018. Plastic waste associated with disease on coral reefs. Science 359 (6374), 460–462. https://doi.org/10.1126/science.aar3320.
Li, Y., Han, D., Sommerfeld, M., Hu, Q., 2011. Photosynthetic carbon partitioning and lipid production in the oleaginous microalga Pseudochlorococcum sp. (Chlorophyceae) under nitrogen-limited conditions. Bioresour. Technol. 102 (1), 123–129. https://doi.org/10.1016/j.biortech.2010.06.036.
Li, S., Wang, P., Zhang, C., Zhou, X., Yin, Z., Hu, T., Hu, D., Liu, C., Zhu, L., 2020a. Influence of polystyrene microplastics on the growth, photosynthetic efficiency and aggregation of freshwater microalgae Chlamydomonas reinhardtii. Sci. Total Environ. 714, 136767. https://doi.org/10.1016/j.scitotenv.2020.136767.
Li, Z., Yi, X., Zhou, H., Chi, T., Li, W., Yang, K., 2020b. Combined effect of polystyrene microplastics and dibutyl phthalate on the microalgae Chlorella pyrenoidosa. Environ. Pollut. 257, 113604. https://doi.org/10.1016/j.envpol.2019.113604.
Li, X., Qiu, H., Zhang, P., Song, L., Romero-Freire, A., He, E., 2023. Role of heteroaggregation and internalization in the toxicity of differently sized and charged plastic nanoparticles to freshwater microalgae. Environ. Pollut. 316, 120517. https://doi.org/10.1016/j.envpol.2022.120517.
Li, X., Chu, Z., Feng, C., Song, P., Yang, T., Zhou, L., Zhao, X., Chai, X., Xing, J., Chen, S., Zhang, J., Wang, J., Liu, G., Tang, H., 2024. Unveiling the molecular mechanisms of size-dependent effect of polystyrene micro/nano-plastics on Chlamydomonas reinhardtii through proteomic profiling. Chemosphere 358, 142220. https://doi.org/10.1016/j.chemosphere.2024.142220.
Liang, J., Niu, T., Zhang, L., Yang, Y., Li, Z., Liang, Z., Yu, K., Gong, S., 2025. Polystyrene microplastics exhibit toxic effects on the widespread coral symbiotic Cladocopium goreaui. Environ. Res. 268, 120750. https://doi.org/10.1016/j.envres.2025.120750.
Lim, Y.A., Khong, N.M.H., Priyawardana, S.D., Ooi, K.R., Ilankoon, I.M.S.K., Chong, M. N., Foo, S.C., 2022. Distinctive correlations between cell concentration and cell size to microalgae biomass under increasing carbon dioxide. Bioresour. Technol. 347, 126733. https://doi.org/10.1016/j.biortech.2022.126733.
Lindeque, P.K., Cole, M., Coppock, R.L., Lewis, C.N., Miller, R.Z., Watts, A.J.R., Wilson-McNeal, A., Wright, S.L., Galloway, T.S., 2020. Are we underestimating microplastic abundance in the marine environment? A comparison of microplastic capture with nets of different mesh-size. Environ. Pollut. 265, 114721. https://doi.org/10.1016/j.envpol.2020.114721.
Liu, G., Jiang, R., You, J., Muir, D.C.G., Zeng, E.Y., 2019. Microplastic impacts on microalgae growth: effects of size and humic acid. Environ. Sci. Technol. 54 (3), 1782–1789. https://doi.org/10.1021/acs.est.9b06187.
Long, M., Paul-Pont, I., Hegaret, H., Moriceau, B., Lambert, C., Huvet, A., Soudant, P., 2017. Interactions between polystyrene microplastics and marine phytoplankton lead to species-specific hetero-aggregation. Environ. Pollut. 228, 454–463. https://doi.org/10.1016/j.envpol.2017.05.047.
Mao, Y., Ai, H., Chen, Y., Zhang, Z., Zeng, P., Kang, L., Li, W., Gu, W., He, Q., Li, H., 2018. Phytoplankton response to polystyrene microplastics: perspective from an entire growth period. Chemosphere 208, 59–68. https://doi.org/10.1016/j.chemosphere.2018.05.170.
Marangoni, L.F.B., Eric, B.A., Ferrier-Pages, C., 2022. Polystyrene nanoplastics impair the photosynthetic capacities of Symbiodiniaceae and promote coral bleaching. Sci. Total Environ. 815, 152136. https://doi.org/10.1016/j.scitotenv.2021.152136.
Niu, T., Yang, Y., Gong, S., Yu, K., Liang, J., 2026. Color disparity enhances the toxic effects of polystyrene microplastics on Cladocopium goreaui. Mar. Pollut. Bull. 222, 118815.
Okubo, N., Takahashi, S., Nakano, Y., 2018. Microplastics disturb the anthozoan-algae symbiotic relationship. Mar. Pollut. Bull. 135, 83–89. https://doi.org/10.1016/j.marpolbul.2018.07.016.
Pinheiro, H.T., MacDonald, C., Santos, R.G., Ali, R., Bobat, A., Cresswell, B.J., Francini-Filho, R., Freitas, R., Galbraith, G.F., Musembi, P., Phelps, T.A., Quimbayo, J.P., Quiros, T.E.A.L., Shepherd, B., Stefanoudis, P.V., Talma, S., Teixeira, J.B., Woodall, L.C., Rocha, L.A., 2023. Plastic pollution on the world's coral reefs. Nature 619 (7969), 311–316. https://doi.org/10.1038/s41586-023-06113-5.
Podbielska, M., Szpyrka, E., 2023. Microplastics-An emerging contaminants for algae. Critical review and perspectives. Sci. Total Environ. 885, 163842. https://doi.org/10.1016/j.scitotenv.2023.163842.
Putnam, H.M., Barott, K.L., Ainsworth, T.D., Gates, R.D., 2017. The vulnerability and resilience of reef-building corals. Curr. Biol. 27 (11), R528–R540. https://doi.org/10.1016/j.cub.2017.04.047.
Qin, L., Xu, Y., Chen, J., Niu, T., Yu, K., Liang, J., 2023. Optimization of in vitro culture method for zooxanthellae associated with reef-building corals. Acta Microbiol Sin. 63 (04), 1658–1671. https://doi.org/10.13343/j.cnki.wsxb.20220656.
Rahman, M.N., Shozib, S.H., Akter, M.Y., Islam, A.R.M.T., Islam, M.S., Sohel, M.S., Kamaraj, C., Rakib, M.R.J., Idris, A.M., Sarker, A., Malafaia, G., 2023. Microplastic as an invisible threat to the coral reefs: sources, toxicity mechanisms, policy intervention, and the way forward. J. Hazard. Mater. 454, 131522. https://doi.org/10.1016/j.jhazmat.2023.131522.
Reichert, J., Schellenberg, J., Schubert, P., Wilke, T., 2018. Responses of reef building corals to microplastic exposure. Environ. Pollut. 237, 955–960. https://doi.org/10.1016/j.envpol.2017.11.006.
Reichert, J., Arnold, A.L., Hoogenboom, M.O., Schubert, P., Wilke, T., 2019. Impacts of microplastics on growth and health of hermatypic corals are species-specific. Environ. Pollut. 254, 113074. https://doi.org/10.1016/j.envpol.2019.113074.
Ripken, C., Khalturin, K., Shoguchi, E., 2020. Response of coral reef dinoflagellates to nanoplastics under experimental conditions suggests downregulation of cellular metabolism. Microorganisms 8 (11), 1759. https://doi.org/10.3390/microorganisms8111759.
Ritchie, R.J., 2006. Consistent sets of spectrophotometric chlorophyll equations for acetone, methanol and ethanol solvents. Photosynth. Res. 89 (1), 27–41. https://doi.org/10.1007/s11120-006-9065-9.
Rochman, C.M., Hentschel, B.T., Teh, S.J., 2014. Long-term sorption of metals is similar among plastic types: implications for plastic debris in aquatic environments. PLoS One 9 (1), e85433. https://doi.org/10.1371/journal.pone.0085433.
Ryckebosch, E., Muylaert, K., Foubert, I., 2012. Optimization of an analytical procedure for extraction of lipids from microalgae. J. Am. Oil Chem. Soc. 89 (2), 189–198. https://doi.org/10.1007/s11746-011-1903-z.
Saad, O.S., Lin, X., Ng, T.Y., Li, L., Ang, P., Lin, S., 2022. Species richness and generalists–specialists mosaicism of symbiodiniacean symbionts in corals from Hong Kong revealed by high-throughput ITS sequencing. Coral Reefs 41, 1–12. https://doi.org/10.1007/s00338-021-02196-6.
Sana, S.S., Dogiparthi, L.K., Gangadhar, L., Chakravorty, A., Abhishek, N., 2020. Effects of microplastics and nanoplastics on marine environment and human health. Environ. Sci. Pollut. Res. 27 (36), 44743–44756. https://doi.org/10.1007/s11356-020-10573-x.
Shruti, V.C., Perez-Guevara, F., Kutralam-Muniasamy, G., 2021. The current state of microplastic pollution in the world’s largest gulf and its future directions. Environ. Pollut. 291, 118142. https://doi.org/10.1016/j.envpol.2021.118142.

Su, Y., Zhang, K., Zhou, Z., Wang, J., Yang, X., Tang, J., Li, H., Lin, S., 2020. Microplastic exposure represses the growth of endosymbiotic dinoflagellate Cladocopium goreaui in culture through affecting its apoptosis and metabolism. Chemosphere 244, 125485. https://doi.org/10.1016/j.chemosphere.2019.125485.

Su, Y., Cheng, Z., Hou, Y., Lin, S., Gao, L., Wang, Z., Bao, R., Peng, L., 2022. Biodegradable and conventional microplastics posed similar toxicity to marine algae Chlorella vulgaris. Aquat. Toxicol. 244, 106097. https://doi.org/10.1016/j.aquatox.2022.106097.

Sun, S., Hu, X., Kang, W., Yao, M., 2023. Combined effects of microplastics and warming enhance algal carbon and nitrogen storage. Water Res. 233, 119815. https://doi.org/10.1016/j.watres.2023.119815.

Szakonyi, D., Byrne, M.E., 2011. Ribosomal protein L27a is required for growth and patterning in Arabidopsis thaliana. Plant J. 65 (2), 269–281. https://doi.org/10.1111/j.1365-313X.2010.04422.x.

Thompson, R.C., Olsen, Y., Mitchell, R.P., Davis, A., Rowland, S.J., John, A.W.G., McGonigle, D., Russell, A.E., 2004. Lost at sea: where is all the plastic? Science 304 (5672), 838. https://doi.org/10.1126/science.1094559.

Thompson, R.C., Courtene-Jones, W., Boucher, J., Pahl, S., Raubenheimer, K., Koelmans, A.A., 2024. Twenty years of microplastics pollution research-what have we learned? Science 386 (6720), eadl2746. https://doi.org/10.1126/science.adl2746.

Torda, G., Donelson, J.M., Aranda, M., Barshis, D.J., Bay, L., Berumen, M.L., Bourne, D. G., Cantin, N., Foret, S., Matz, M., Miller, D.J., Moya, A., Putnam, H.M., Ravasi, T., van Oppen, M.J.H., Thurber, R.V., Vidal-Dupiol, J., Voolstra, C.R., Watson, S.-A., Whitelaw, E., Willis, B.L., Munday, P.L., 2017. Rapid adaptive responses to climate change in corals. Nat. Clim. Chang. 7 (9), 627–636. https://doi.org/10.1038/nclimate3374.

Venn, A.A., Loram, J.E., Douglas, A.E., 2008. Photosynthetic symbioses in animals. J. Exp. Bot. 59 (5), 1069–1080. https://doi.org/10.1093/jxb/erm328.

Wang, W., Liu, H., Liu, H., Chen, J., Xu, X., Xia, J., Zhang, P., 2023. Effects of polystyrene microparticles on growth and physiological metabolism of microalgae Scendesmus obliquus. Sustainability 15 (14), 11223. https://doi.org/10.3390/su151411223.

Wu, Y., Guo, P., Zhang, X., Zhang, Y., Xie, S., Den, J., 2019. Effect of microplastics exposure on the photosynthesis system of freshwater algae. J. Hazard. Mater. 374, 219–227. https://doi.org/10.1016/j.jhazmat.2019.04.039.

Wu, D., Wang, T., Wang, J., Jiang, L., Yin, Y., Guo, H., 2021. Size-dependent toxic effects of polystyrene microplastic exposure on Microcystis aeruginosa growth and microcystin production. Sci. Total Environ. 761, 143265. https://doi.org/10.1016/j.scitotenv.2020.143265.

Xiao, Y., Jiang, X., Liao, Y., Zhao, W., Zhao, P., Li, M., 2020. Adverse physiological and molecular level effects of polystyrene microplastics on freshwater microalgae. Chemosphere 255, 126914. https://doi.org/10.1016/j.chemosphere.2020.126914.

Xu, Y., Peng, B.-Y., Zhang, X., Xu, Q., Yang, L., Chen, J., Zhou, X., Zhang, Y., 2024. The aging of microplastics exacerbates the damage to photosynthetic performance and bioenergy production in microalgae Chlorella pyrenoidosa. Water Res. 259, 121841. https://doi.org/10.1016/j.watres.2024.121841.

Yang, L., Su, Q., Si, B., Zhang, Y., Zhang, Y., Yang, H., Zhou, X., 2022. Enhancing bioenergy production with carbon capture of microalgae by ultraviolet spectrum conversion via graphene oxide quantum dots. Chem. Eng. J. 429, 132230. https://doi.org/10.1016/j.cej.2021.132230.

Ye, S., Rao, M., Xiao, W., Zhou, J., Li, M., 2023. The relative size of microalgal cells and microplastics determines the toxicity of microplastics to microalgae. Process. Saf. Environ. Prot. 169, 860–868. https://doi.org/10.1016/j.psep.2022.11.077.

Yemm, E.W., Willis, A.J., 1954. The estimation of carbohydrates in plant extracts by anthrone. Biochem. J. 57 (3), 508–514. https://doi.org/10.1042/bj0570508.

Zhang, C., Li, Q., Fu, L., Zhou, D., Crittenden, J.C., 2018. Quorum sensing molecules in activated sludge could trigger microalgae lipid synthesis. Bioresour. Technol. 263, 576–582. https://doi.org/10.1016/j.biortech.2018.05.045.

Zhang, W., Ok, Y.S., Bank, M.S., Sonne, C., 2023. Macro-and microplastics as complex threats to coral reef ecosystems. Environ. Int. 174, 107914. https://doi.org/10.1016/j.envint.2023.107914.

Zhao, Z., Zheng, X., Han, Z., Li, Y., He, H., Lin, T., Xu, H., 2024. Polystyrene microplastics enhanced the effect of PFOA on Chlorella sorokiniana: perspective from the cellular and molecular levels. J. Hazard. Mater. 465, 133455. https://doi.org/10.1016/j.jhazmat.2024.133455.

Zhu, J., Cai, Y., Wakisaka, M., Yang, Z., Yin, Y., Fang, W., Xu, Y., Omura, T., Yu, R., Zheng, A.L.T., 2023. Mitigation of oxidative stress damage caused by abiotic stress to improve biomass yield of microalgae: a review. Sci. Total Environ. 896, 165200. https://doi.org/10.1016/j.scitotenv.2023.165200.